



# **Détection et prévention du fonctionnement des génératrices diesel à faible charge par les réseaux de neurones artificiels**

Mémoire présenté

dans le cadre du programme de maîtrise en ingénierie

en vue de l'obtention du grade de maître ès sciences appliquées (M. Sc. A.)

PAR

© **Milad Ghorbanzadeh**

**Février 2024**



**Composition du jury :**

**Noureddine Barka, président du jury, UQAR**

**Adrian Ilinca, directeur de recherche, UQAR**

**Mohamad Issa, codirecteur de recherche, IMQ**

**Fahed Martini, examinateur externe, ÉTS**

Dépôt initial le 27 novembre 2023

Dépôt final le 15 février 2024



UNIVERSITÉ DU QUÉBEC À RIMOUSKI  
Service de la bibliothèque

Avertissement

La diffusion de ce mémoire ou de cette thèse se fait dans le respect des droits de son auteur, qui a signé le formulaire « *Autorisation de reproduire et de diffuser un rapport, un mémoire ou une thèse* ». En signant ce formulaire, l'auteur concède à l'Université du Québec à Rimouski une licence non exclusive d'utilisation et de publication de la totalité ou d'une partie importante de son travail de recherche pour des fins pédagogiques et non commerciales. Plus précisément, l'auteur autorise l'Université du Québec à Rimouski à reproduire, diffuser, prêter, distribuer ou vendre des copies de son travail de recherche à des fins non commerciales sur quelque support que ce soit, y compris Internet. Cette licence et cette autorisation n'entraînent pas une renonciation de la part de l'auteur à ses droits moraux ni à ses droits de propriété intellectuelle. Sauf entente contraire, l'auteur conserve la liberté de diffuser et de commercialiser ou non ce travail dont il possède un exemplaire.



## **ACKNOWLEDGEMENT**

I extend my deepest gratitude to my supervisor, Professor Adrian Ilinca, a person of exceptional integrity, for the unwavering support and invaluable guidance he provided. His acceptance of me as one of the master's students on his esteemed team has been an honor. Additionally, I would like to thank Dr. Mohamad Issa for his constant guidance, support, and exceptional feedback.

To my beloved wife, your steadfast support and continuous encouragement throughout my years of study have been my pillars. Your presence in this journey has been a source of strength and inspiration, for which I am profoundly grateful.

I also want to acknowledge my friends and the entire community at UQAR University. The camaraderie and collaborative spirit among colleagues and employees have enriched my academic experience.



## RÉSUMÉ

Électrifier les régions éloignées qui n'ont pas accès au réseau électrique national dépend fortement des générateurs diesel. Cependant, un défi majeur se pose lorsque la demande en électricité est faible, ce qui nécessite que le moteur diesel fonctionne sous un faible régime. Une combustion inadéquate pendant cette phase entraîne une accumulation significative de polluants à l'intérieur du cylindre, ce qui peut affecter négativement le fonctionnement du moteur.

L'objectif principal de cette recherche est d'optimiser le fonctionnement d'un groupe électrogène diesel en détectant et en prévenant son fonctionnement sous un faible régime grâce à la mise en œuvre d'un système de contrôle basé sur des Réseaux de Neurones Artificiels (RNA). Les expériences ont été réalisées sur un moteur à allumage par compression Caterpillar de 8,8 litres d'une puissance maximale de 300 kW et les données respectives sur les gaz d'échappement ont été collectées à l'aide d'un analyseur de gaz de combustion.

Les données acquises ont été utilisées pour entraîner un réseau neuronal capable d'identifier les schémas lorsque le groupe électrogène diesel fonctionne en dessous de la charge de fonctionnement prescrite par le fabricant, soit dans notre cas, en dessous de 35 %. À cette fin, différentes architectures de réseaux neuronaux ont été testées pour déterminer la structure la plus optimale adaptée à notre donnée d'entrée produisant la prédiction la plus précise de la charge de fonctionnement du GED. La charge de fonctionnement prédite est ensuite utilisée dans un système de contrôle pour déterminer la valeur de la résistance requise du banc de charge qui doit être chargée sur l'unité génératrice du GED. Cela permettrait de convertir l'énergie électrique en chaleur, améliorant ainsi l'état de fonctionnement du GED en atténuant les impacts négatifs de son fonctionnement à faible charge.

Les résultats de simulation acquis de cette recherche démontrent que le système de contrôle développé détecte la sous-performance d'un GED avec une précision remarquable,

dont le coefficient de corrélation et la Racine de l'Erreur Quadratique Moyenne (REQM) sont proches de 0,007 et 0,03 pour les données d'entraînement et de test, respectivement.

Mots clés : [faible charge; sous-performance; générateur diesel; moteur à combustion; production d'électricité autonome ; optimisation ; Réseau de Neurones Artificiels (RNA)]

## ABSTRACT

Electrifying remote regions lacking access to the national electricity grid relies heavily on diesel generators. However, a significant challenge arises when the electricity demand is low, necessitating the diesel engine to operate under a low-load regime. Inadequate combustion during this phase results in a significant accumulation of pollutants inside the cylinder, adversely affecting the engine's operation.

The main objective of this research is to optimize the operation of a diesel generator by detecting and preventing its low-load operation by implementing a control system based on Artificial Neural Networks (ANN). The experiments were carried out on an 8.8-liter Caterpillar compression ignition engine with a maximum power of 300 kW, and the respective exhaust gas data were collected using a gas combustion analyzer.

The acquired data was used to train a neural network capable of identifying patterns when the diesel generator set operates below the manufacturer's prescribed operating load, which, in our case, is below 35%. For this purpose, different neural network architectures were tested to determine the most optimal structure adapted to our input data, producing the most accurate prediction of the operating load of the diesel engine generator (DEG). The predicted DEG operating load is then used in a control system to determine the required load bank resistance value that should be loaded onto DEG's generator unit. This will convert electrical energy into heat, thereby improving the DEG's operating state by mitigating its low-load operation's negative impacts.

The simulation results acquired from this research demonstrate that the developed control system detects the underperformance of a DEG with remarkable accuracy, whose correlation coefficient, and Root Mean Squared Error (RMSE) are close to 0.007 and 0.03 for training and testing data, respectively.

*Keywords:* [low load; underperformance; diesel generator; combustion engine; stand-alone power generating; optimization; Artificial Neural Networks]



## TABLE OF CONTENTS

ACKNOWLEDGEMENT .....	vii
RÉSUMÉ .....	ix
ABSTRACT.....	xi
TABLE OF CONTENTS.....	xiii
LIST OF TABLES.....	xv
LIST of FIGURES .....	xvii
LIST OF ABBREVIATIONS, INITIALS AND ACRONYMS .....	xix
LIST of SYMBOLS.....	xxi
CHAPTER 1: INTRODUCTION.....	1
1.1 BACKGROUND AND LITERATURE REVIEW .....	1
1.2 PROBLEM ANALYSIS .....	3
1.2.1 Low-load operation.....	4
1.3 RESEARCH OBJECTIVE .....	6
1.4 RESEARCH METHODOLOGY .....	7
1.5 THESIS STRUCTURE .....	8
CHAPTER 2 ARTICLE .....	11
CHAPTER 3: COMPARATIVE ANALYSIS OF ANN MODELS IN INDUSTRIAL CONTROL SYSTEMS.....	29
3.1 ANN JUSTIFICATION.....	29
3.2 ANN CLASSIFICATION AND COMPARISON.....	30
3.2.1 Learning Algorithm .....	30
3.2.2 ANN Architecture.....	33
CHAPTER 4: DESIGN AND IMPLEMENTATION OF ANN ALGORITHMS FOR DIESEL GENERATOR OPTIMIZATION.....	37

4.1 INTRODUCTION .....	37
4.2 NEURAL NETWORK ARCHITECTURE SELECTION.....	37
4.3 ANN MODELING .....	38
4.3.1 Selection of input and output parameters.....	40
4.3.2 Data normalization.....	41
4.3.3 Statistical assessment of output parameters.....	41
4.3.4 Data Allocation Ratio Selection.....	42
4.4 THE ANN ARCHITECTURE .....	44
4.4.1 Execution of the MLP network model.....	45
4.4.2 Modification of the MLP Structure.....	49
4.4.3 Results of the MLP Network .....	52
4.4.4 Execution of the RBF network model .....	56
4.4.5 Modification of the RBF network.....	57
4.4.6 Results of the RBF network.....	58
CHAPTER 5: RESULTS AND DISCUSSIONS .....	63
5.1 APPLICATION OF THE PROPOSED NETWORK FOR DEG OPTIMIZATION .....	63
5.1.1 Scenario 1.....	66
5.1.2 Scenario 2.....	67
CHAPTER 6: CONCLUSIONS .....	69
6.1 SUMMARY AND CONCLUSIONS.....	69
6.2 THE LIMITATIONS OF THE MODEL, RECOMMENDATIONS, AND FUTURE RESEARCH .....	72
BIBLIOGRAPHIC REFERENCES .....	73

## LIST OF TABLES

Table 1 Load levels represented as a percentage of the maximum power rating (Tufte, 2014) .....	3
Table 2 Consequences of operating a fixed-speed diesel-electric generator at a low load (Issa et al., 2020; Mustayen et al., 2022).....	5
Table 3 Network's performance for different dataset ratio allocation in MLP neural network.....	43
Table 4 Network's performance for different dataset ratio allocation in RBF neural network.....	44
Table 5 Training algorithms and their corresponding function in MATLAB .....	49
Table 6 MLP model Evaluation using different training functions. ....	50
Table 7 Network's performance for different numbers of hidden neurons .....	52
Table 8 Network attributes generated on MATLAB .....	52
Table 9 RBF network result with different spread coefficients.....	58
Table 10 RMSE and $R^2$ comparison between MLP and RBF for DEG operating load prediction.....	63
Table 11 Exhaust gas data from DEG operating at 24% of nominal power capacity. ....	67
Table 12 Exhaust gas data from DEG operating at 38% of nominal power capacity .....	67



## LIST OF FIGURES

Figure 1 Diesel use for electricity generation was studied in 213 isolated Canadian communities (Royer, 2011).....	2
Figure 2 Neural Network Architecture selection procedure .....	39
Figure 3 FFNN architecture used in this study .....	40
Figure 4 MSE comparison of the two neural networks for different training ratios .....	45
Figure 5 MATLAB neural network fitting tools .....	46
Figure 6 The block diagram in an MLP network implemented by MATLAB.....	47
Figure 7 The structure of the implemented MLP neural network in MATLAB software. ....	48
Figure 8 RMSE and coefficient of correlation for different numbers of neurons in MLP network. ....	53
Figure 9 Performance plot of the MLP neural network.....	54
Figure 10 Regression plot of the ANN predicted operating load and the actual load value using MLP neural network. ....	55
Figure 11 Training state of the MLP network .....	56
Figure 12 RMSE and coefficient of correlation for predicting the operating load in RBF network .....	59
Figure 13 RBF network performance in different iterations .....	60
Figure 14 Regression plot of the ANN predicted operating load and the actual load value using RBF neural network.....	60
Figure 15 Training state of the RBF network .....	61
Figure 16 Data acquisition for the neural network .....	64
Figure 17 Resistive load bank control .....	64
Figure 18 Optimization flow chart for our diesel engine generator .....	65
Figure 19 DEG Underperformance optimization schematic .....	65



## LIST OF ABBREVIATIONS, INITIALS AND ACRONYMS

<b>GHG</b>	Greenhouse Gases
<b>RES</b>	Renewable Energy Source
<b>DEG</b>	Diesel Engine Generator
<b>DG</b>	Diesel Generator
<b>ANN</b>	Artificial Neural Network
<b>BP</b>	Back Propagation
<b>BPA</b>	Back Propagation Algorithm
<b>CNN</b>	Cellular Neural Network
<b>MLP</b>	Multilayered Perceptron
<b>RBF</b>	Radial Basis Function
<b>RBFN</b>	Radial Basis Function Network
<b>FFNN</b>	Feedforward Neural Network
<b>MSE</b>	Mean Squared Error
<b>RMSE</b>	Root Mean Squared Error
<b>MAE</b>	Mean Absolute Error
<b>SO<sub>2</sub></b>	Sulfur Dioxide
<b>CO<sub>2</sub></b>	Carbon Dioxide
<b>NO<sub>x</sub></b>	Nitrogen Oxide
<b>O<sub>2</sub></b>	Oxygen

<b>CO</b>	Carbon Monoxide
<b>S</b>	Sulfur
<b>PM</b>	Particulate Matter
<b>PPM</b>	Parts Per Million
<b>ULSD</b>	Ultra-Low Sulfur Diesel
<b>BSFC</b>	Break-Specific Fuel Consumption
<b>LM</b>	Levenberg-Marquardt

## LIST OF SYMBOLS

$w$	Neural network weights
$b$	Neural network offset
$\varphi$	Gaussian function
$c$	Center vector
$\sigma$	Width parameter (Spread)
$R$	Correlation coefficient
$R^2$	Coefficient of determination



## CHAPTER 1: INTRODUCTION

### 1.1 BACKGROUND AND LITERATURE REVIEW

The electrification of isolated regions has always been one of the significant challenges for both governments and utility companies. As stated by the World Bank, most of the 1.2 billion people worldwide without access to electricity reside in Africa and Asia (Arriaga et al., 2014). Extending the power grid to isolated locations is expensive and technically complex (Akbas et al., 2022). Consequently, these regions predominantly rely on diesel generators for energy generation, owing to their excellent reliability, stability, extended service life, and ease of production (Issa et al., 2020). In Canada, over 280 communities, approximately 200,000 people, one-third of whom are situated in northern territories (Yukon, Nunavut, etc.), are not connected to the electrical grid. These remote regions primarily rely on diesel for electricity production, as depicted in Figure 1. This choice is driven by the reliability of this energy source and the fact that local utilities are better familiar with this energy generation technology, as well as the diesel's high energy density and ease of storage. (McFarlan, 2018). On the other hand, diesel generators are relatively affordable, easy to install, and can be scaled up to meet the load profile of isolated regions (CER, 2018). That is why, as per the Remote Communities Energy Database of Natural Resources Canada, more than 70% of remote communities opt for diesel generators to be self-sufficient in their energy production. Diesel fuel remains the primary choice for remote and autonomous energy networks such as agricultural, farming, and fishing facilities, telecommunication towers, weather forecasting systems, as well as exploration and extraction mining sites which are not connected to the local or national distribution and transmission electricity network (Canada, 2018; Rezkallah, 2016).

Despite many advantages, diesel generators can cause various socioeconomic, technical, and environmental issues responsible for the emission of significant greenhouse gases (GHGs) worldwide. For this reason, governments plan to reduce reliance on off-grid power systems using petroleum products. One alternative for these remote regions is the

hybridization of Diesel engines with renewable energy sources because RESs are unpredictable, intermittent, and dependent on meteorological conditions, which makes them unreliable to be used alone for off-grid electricity generation (Djelailia et al., 2019). Diesel engines hybridized with other energy sources, such as wind turbines or photovoltaic farms, can reduce energy production costs in isolated regions and offset carbon emissions (Memon & Patel, 2021)

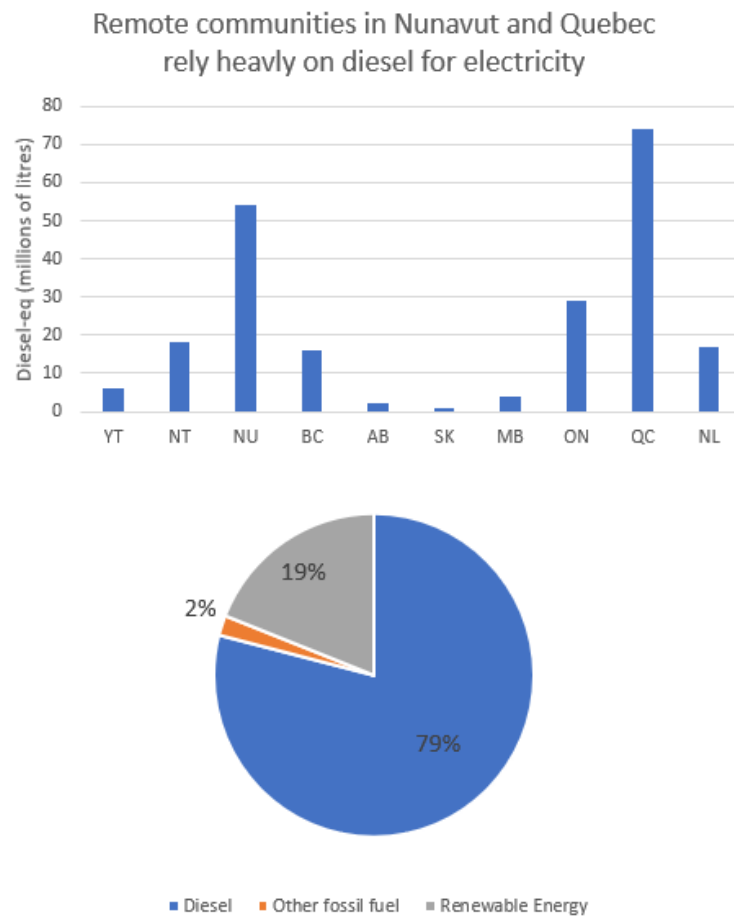


Figure 1 Diesel use for electricity generation was studied in 213 isolated Canadian communities (Royer, 2011).

## 1.2 PROBLEM ANALYSIS

The use of diesel engine generators (DEG) for electricity production in isolated regions, either used alone or in conjunction with Renewable Energy Sources (RES), poses various technical problems, the most important of which is the underperformance of diesel engine generator (DEG), which occurs when the generator operates below a certain threshold especially, for an extended period (over 30 min). This phenomenon can result in the degradation of the engine over time and its frequent maintenance, which would consequently increase energy production costs and reduce the network's reliability. According to Caterpillar experts, a DEG operating at any load under 30% of its nominal power is considered operating at a low-load operation (Jabeck, 2013). However, other research by Det Norske Veritas and Germanischer Lloyd (DNV-GL) indicates 40% of the maximum power as the threshold for DEG's underperformance and the range between 40-80% as the normal and recommended operating power (Tuftte, 2014). Table 1 provides the framework for the entire load range of a DEG. In the following section, we review and explain the origin of DEGs' operational deterioration in detail.

Table 1 Load levels represented as a percentage of the maximum power rating (Tuftte, 2014)

<b>Power percentage</b>	<b>Load level</b>
0-25%	Very low load
26-39%	Low load
40-80%	Regular load
81-90%	High load
91-100%	Very high load

### 1.2.1 Low-load operation

One of the operational challenges concerning DEGs is their performance at a steady speed to produce reliable AC power with a constant voltage profile, which is then distributed to various consumers. However, electrical energy demand and energy production of renewable energy resources fluctuate instantaneously, making them unpredictable in demand-side management. In addition, in remote areas, diesel engine generators are designed larger than necessary to accommodate peak demand, which can be four or five times greater than the average electrical load (Mobarra et al., 2022). This would inevitably lead to the operation of diesel generators at reduced loads, especially for extended periods, causing the degradation of its technical parts and condensation of combustion residues on the cylinder walls. This would increase friction and fuel consumption in the DEG and decrease its efficiency, resulting in premature wear of the diesel generator (German-Galkin et al., 2020; Issa et al., 2020). DEGs also face the operational challenge of being predominantly fixed speed, resulting in extended periods of running in low loads, typically between 0-25% of their nominal power (as indicated in Table 1). This prolonged operation at low loads increases oil consumption. Subsequently, it leads to a more significant accumulation of carbonized oil or oil residue within the engine and in the intake and exhaust systems. (Issa et al., 2020). The presence of these residues adversely impacts the engine's longevity and operational performance, thereby leading to an increase in its upkeep frequency (Jabeck, 2013).

Moreover, when an engine operates at low loads, it experiences cooling, leading to incomplete fuel combustion and the emission of white smoke containing substantial hydrocarbons (Mustayen et al., 2021). Consequently, the low fuel temperature causes an increase in incomplete combustion within the oil. Insufficient dilation of the piston and its rings and the cylinder results in the oil level rising and leaking through the exhaust valves. As the diesel oil infiltrates the crankcase, it inevitably deteriorates the lubricants' quality (Penny & Jacobs, 2016). Increased engine speed until the operating temperature is attained is one technique to address this issue and eliminate these deposits. Load banks are widely adopted within the industrial sector, particularly in the United States, to mitigate these

adverse consequences (German-Galkin et al., 2020). On the contrary, by integrating several small fixed-speed diesel-electric generators, with their combined power output matching that of a single large, fixed diesel-electric generator, it becomes possible to prevent the large engine from operating under low-load conditions (Ayodele et al., 2017).

Table 2 provides a detailed account of how the performance of a fixed-speed diesel-electric generator set is influenced by its underperformance, highlighting the resulting consequences.

Table 2 Consequences of operating a fixed-speed diesel-electric generator at a low load (Issa et al., 2020; Mustayen et al., 2022)

<b>Phenomenon</b>	<b>Indicator</b>	<b>Causes and implications</b>
Wet stacking	- A dark fluid resembling engine oil streaming from the exhaust pipe or turbocharge.	Due to the engine's extended operation at low loads, the temperature falls short of the required value for achieving complete fuel combustion.
	- Moist black liquid near the exhaust manifold of the engine	
Cylinder polishing	- Increased oil consumption	Mechanical friction is caused by carbon deposits surrounding the rings, which arise from incomplete fuel combustion of the engine operating at low loads.
	- Power reduction	
Cylinder glazing	- Increased oil consumption	- Cold start of the engine
	- Power reduction	
	- Engine emissions	- The frequent need for added oil

---

	- Engine underload operation
--	------------------------------

---

Consequences	<ul style="list-style-type: none"> <li>- Expenses: The frequent appearance of these phenomena diminishes the engine's lifespan and primary components significantly. Moreover, they result in higher fuel consumption, leading to increased expenses.</li> <li>- Pollution: Elevated levels of engine emissions</li> <li>- Power: Decrease in the engine's maximum power output compared to its rate power.</li> <li>- Upkeep: A fixed-speed engine encountering these issues needs more frequent maintenance than an engine working under the manufacturer's prescribed load.</li> </ul>
--------------	---

---

### 1.3 RESEARCH OBJECTIVE

The primary goal of this project is to develop an artificial neural network-based algorithm by choosing the best configuration among different ANN models to analyze the exhaust emission data and fuel consumption for a diesel generator operating at an ambient temperature of 21°C in order to detect and avoid its underperforming operation in advance. For this purpose, a few specific objectives will be pursued in this research, including:

- Data acquisition of exhaust emission gases, operating temperature, and fuel consumption of the DEG under different loading conditions.
- Identifying the best input data to train the neural network, indicative of DEG underperformance, to train our neural network effectively.

- Identifying the optimal configuration for an ANN architecture capable of accurately predicting the underperformance of a DEG in a timely manner.
- Developing a control system based on the developed ANN architecture that would add required resistive loads to the generator part of DEG to prevent its underperformance.

#### **1.4 RESEARCH METHODOLOGY**

This research experiment was performed under a consistent engine speed of 1800 revolutions per minute. Ultra-low sulfur diesel fuel (ULSD) designed for off-road engines (such as locomotive and vessel diesel engines), which contains 15 parts per million (ppm) of sulfur and adheres to the prevailing standard set by Environment Canada for all engine diesel fuel, was utilized for the tests (Canada, 2006). The loads were adjusted within the 0 to 130 kilowatts range, equivalent to 0-52% of the generator's maximum capacity. This was done to replicate the electrical demand pattern in an isolated microgrid located in northern Quebec. All assessments were carried out under a consistent ambient temperature of 21°C. Readings were recorded for each load once the engine achieved a stable operational state. The subsequent experimental parameters were identified:

- Exhaust emission attributes include the temperature of the emitted gas after combustion, SO<sub>2</sub>, CO<sub>2</sub>, NO<sub>x</sub>, O<sub>2</sub>, CO, and S.
- The impact of Brake-Specific Fuel Consumption (BSFC)

The measurements were repeated three times for very low load (0-25%), low load (26-39%), and regular load (40-52%). The tests were conducted under the ISO 3046-1:2002 standard, which involved adjusting the load power and fuel consumption results to standard conditions. Subsequently, each measured parameter is examined to ascertain its consistency under low-load conditions. This analysis aims to pinpoint the most relevant indicators of engine underperformance within our measurement process that can be used for training our neural network. Upon selecting the best input values for our neural network, the next step

involves preprocessing the data, which includes normalization through the min-max normalization equation. The next step involves dataset allocation ratio selection for train, test, and validation data and evaluating the model's performance on different splits using appropriate metrics to find the best data split. Training the neural network is done through MATLAB software neural network fitting tool, and the achievement of the optimal topological structure is done through a heuristic approach by evaluation of the ANN model's performance by considering the coefficient of determination ( $R^2$ ) and mean squared error (MSE) as evaluative metrics. The network is then fine-tuned by changing its different hyperparameters, including its learning algorithm, activation functions, number of hidden layers, etc., to find the optimal network configuration that can later be used in our control system.

## **1.5 THESIS STRUCTURE**

Following the introductory first chapter, which outlines the background, research objectives, and methodology, the structure of this thesis progresses as follows:

Chapter 2 of this research features an article published in a peer-reviewed scientific journal titled "Experimental Underperformance Detection of a Fixed-Speed Diesel-Electric Generator Based on Exhaust Gas Emissions." This article delves into the initial two objectives established in Chapter 1, focusing on acquiring data related to exhaust emission gases and other attributes of the Diesel-Electric Generator (DEG). The subsequent step involves identifying the most pertinent input data for training our neural network.

Chapter 3 delves into analyzing the commonly used Artificial Neural Network (ANN) models within industrial control systems. The aim is to assess and refine the selection process, ultimately pinpointing the most pertinent alternatives that align with this research's specific scope and objectives.

Chapter 4 of this research delves into an exploration of an algorithm built upon the selected ANN architectures outlined in Chapter 3. The focus is on configuring and fine-tuning the hyperparameters of the network to develop the most accurate prediction algorithm.

Chapter 5 centers on analyzing the obtained results and their practical implementation in the control system to avert engine underperformance.

Chapter 6 serves as the concluding segment of this thesis; the emphasis is placed on summarizing the key findings of the research and exploring potential avenues for future work.



## CHAPTER 2

### Article

Experimental Underperformance Detection of a Fixed-Speed Diesel-Electric Generator  
Based on Exhaust Gas Emissions

Published in Journal of *Energies* 2023, 16, 3537.

<https://doi.org/10.3390/en16083537>

### Résumé

Cet article se concentre sur l'analyse des performances et des émissions d'un moteur diesel multicylindre à vitesse fixe alimentant un générateur électrique de 300 kW, utilisant du diesel à très faible teneur en soufre ( $\leq 15$  mg/kg), pour fournir de l'énergie dans une communauté canadienne isolée. Faire fonctionner un moteur diesel à faible charge ( $\leq 30$  %) pose un défi important pour les générateurs électriques diesel à vitesse fixe. Une combustion incomplète dans cette phase entraîne une accumulation notable de contaminants dans le cylindre, entraînant divers problèmes chimiques et mécaniques pour le moteur diesel. Ces problèmes incluent la friction, une efficacité réduite, une consommation de carburant accrue et une panne prématurée du générateur, collectivement classés comme sous-performances, et divers signes sont attribués, notamment une diminution de la puissance de sortie, une consommation de carburant accrue et un bruit ou des vibrations anormaux du moteur. Par conséquent, la détection et la prévention rapides des sous-performances et la minimisation de leur fonctionnement prolongé sont des objectifs impératifs de cette étude.

Cette étude vise à combler une lacune notable en matière de recherche liée à l'identification des sous-performances basées sur les émissions de gaz, en particulier dans les générateurs diesel à vitesse fixe dans les communautés isolées qui n'ont pas accès à des carburants propres. La plupart des générateurs de ces communautés sont surdimensionnés et fonctionnent principalement à faible charge, ce qui entraîne une consommation accrue de pétrole et des gisements de pétrole carbonisés.

Les tests de cette étude ont été réalisés à un régime moteur de 1 800 tr/min, avec du carburant diesel à très faible teneur en soufre conforme aux normes d'Environnement Canada. Les variations de charge de 0 à 156 kW reproduisaient le profil de charge électrique dans un micro-réseau isolé. Les paramètres expérimentaux, notamment les émissions d'échappement et la consommation de carburant spécifique aux freins (BSFC), ont été enregistrés dans des conditions de charge très faibles (0 à 25 %), faibles (26 à 39 %) et normales (40 à 52 %), conformément à la norme ISO. Norme 3046-1:2002 sous une température ambiante de 21°C. Les paramètres expérimentaux suivants ont été déterminés lors des tests :

1. Caractéristiques des émissions d'échappement, notamment la température des gaz d'échappement, le SO<sub>2</sub>, le CO<sub>2</sub>, le NO<sub>x</sub>, l'O<sub>2</sub>, le CO et le S.

2. L'effet de la consommation de carburant spécifique aux freins (BSFC)

Cette étude montre que la température des gaz d'échappement est un indicateur de sous-performance précieux, se stabilisant à 220°C sous 30 % de charge. La consommation de carburant spécifique aux freins (BSFC) peut également servir d'indice de sous-performance, montrant une consommation accrue lors de faibles charges prolongées ( $\leq 30\%$ ). En ce qui concerne les émissions de gaz, le dioxyde de carbone, l'oxyde d'azote et le soufre présentaient des niveaux élevés lorsque le générateur fonctionnait en dessous de la moyenne, ce qui en faisait des indicateurs fiables de sous-performance. Cependant, le monoxyde de carbone et le dioxyde de soufre ne constituaient pas de très bons indicateurs, car leurs valeurs d'émission étaient similaires sous des charges faibles et normales.

Article

# Experimental Underperformance Detection of a Fixed-Speed Diesel–Electric Generator Based on Exhaust Gas Emissions

Milad Ghorbanzadeh <sup>1</sup>, Mohamad Issa <sup>2</sup> and Adrian Ilinca <sup>3,\*</sup>

<sup>1</sup> Department of Mathematics, Computer Science and Engineering, Université du Québec à Rimouski, 300 Allée des Ursulines, Rimouski, QC G5L 3A1, Canada; milad.ghorbanzadeh@uqar.ca

<sup>2</sup> Department of Applied Sciences, Quebec Maritime Institute, Rimouski 53 Rue St Germain O, Rimouski, QC G5L 4B4, Canada; missa@imq.qc.ca

<sup>3</sup> Mechanical Engineering Department, École de Technologie Supérieure, 1100 Notre-Dame St W, Montréal, QC H3C 1K3, Canada

\* Correspondence: adrian.ilinca@etsmtl.ca; Tel.: +1-514-396-8800 (ext. 8405)

**Abstract:** Low load is one of the most challenging combustion stages for a fixed-speed diesel electric generator. Due to incomplete combustion during this phase, a significant proportion of contaminants form inside the cylinder. This can lead to numerous chemical and mechanical harms to the diesel engine, resulting in friction, efficiency reduction, increased fuel consumption, and prematurely ending the generator's life. These phenomena are qualified as underperformance, possibly due to a misfire and/or a low-efficiency value (air fuel–fuel ratio). Therefore, detecting and preventing underperformance and reducing its extended operation is crucial. This paper deals with the performance and emission analysis of a multicylinder fixed-speed diesel engine driving an electric generator (300 kW) fueled with ultra-low sulfur diesel ( $\leq 15$  mg/kg) to provide energy in an isolated Canadian community. The tests were carried out according to ISO 3046-1:2002 standard in a remote site to identify clues that can prevent prolonged operation in underperformance. Among the tests conducted, emissions such as sulfur (S), carbon dioxide (CO<sub>2</sub>), nitrogen oxide (NO<sub>x</sub>), and exhaust gas temperature are considered the best indices for detecting the underperformance of a fixed-speed diesel–electric generator under very-low and low load (0–30%) with the following registered values: 18 ppm for S, 4% for CO<sub>2</sub>, 150 ppm for NO<sub>x</sub>, and 210 °C for the temperature.

**Keywords:** low load; exhaust gas temperature; underperformance; brake-specific fuel consumption; diesel generator; sulfur emission; nitrogen oxide emission; carbon dioxide emission



**Citation:** Ghorbanzadeh, M.; Issa, M.; Ilinca, A. Experimental Underperformance Detection of a Fixed-Speed Diesel–Electric Generator Based on Exhaust Gas Emissions. *Energies* **2023**, *16*, 3537. <https://doi.org/10.3390/en16083537>

Academic Editors: Adonios Karpetsis and Constantine D. Rakopoulos

Received: 9 March 2023

Revised: 13 April 2023

Accepted: 18 April 2023

Published: 19 April 2023



**Copyright:** © 2023 by the authors. Licensee MDPI, Basel, Switzerland. This article is an open access article distributed under the terms and conditions of the Creative Commons Attribution (CC BY) license (<https://creativecommons.org/licenses/by/4.0/>).

## 1. Introduction

Underperformance is when an engine is not producing the expected or desired level of power output, regardless of its operating speed [1–3]. The low regime, on the other hand, refers specifically to low engine speeds or revolutions per minute (RPM) [4]. While underperformance and the low regime are often associated, they are not necessarily the same. An engine can be underperforming at any RPM, including high RPMs. For example, an engine may produce less power than expected due to a mechanical issue, such as a worn piston ring, regardless of operating speed [5]. Conversely, an engine may be operating at low RPMs without necessarily underperforming. This could be intentional during a time of load transition, for example, onboard ships or in rail transport, when the diesel–electric generators operate under low load ( $\leq 30\%$ ) but for a determined time (less than 30 min) [6–9]. According to the Caterpillar manufacturer, underperformance occurs when the diesel generator operates under low load ( $\leq 30\%$ ) for an extended period (over 30 min) and frequently. Furthermore, if the engine is not producing enough power to meet the output demands, it may be considered underperforming even at low RPMs.

According to [10], the underperformance of diesel engines at low regime operation is due to a few factors. First, diesel engines operate by compressing air to a high temperature

and pressure before injecting fuel, igniting, and driving the piston. At low engine speeds, the air compression is not as effective and the fuel may not ignite as efficiently, leading to incomplete combustion and reduced power output. Additionally, at low engine speeds, the engine's turbocharger may not be spinning fast enough to provide sufficient airflow to the engine, resulting in a lack of power [11]. This is because turbochargers rely on the engine's exhaust gas flow to drive a turbine that compresses incoming air. As a result, the exhaust gas flow is reduced at low engine speeds, resulting in less boost pressure and reduced power output.

Furthermore, diesel engines often have a narrow power band, meaning their optimal operating range is relatively narrow [12]. Therefore, the engine may not operate within this optimal range at low speeds, reducing power output and efficiency [13]. Table 1 describes the causes and consequences of the prolonged low-load operation on a fixed-speed diesel-electric generator performance.

Today, there are a few ways to detect the underperformance of an engine. According to [14], the most apparent sign of underperformance is a decrease in power output. Additionally, fuel consumption, engine noise, and/or vibration can be signs of underperformance. Regular maintenance and inspection can also help prevent underperformance by identifying and fixing issues before they become significant problems [15].

**Table 1.** Effects of fixed-speed diesel–electric generator light load running [16–18].

Phenomena	Signs of Occurrence	Causes/Consequences
Wet stacking	<ul style="list-style-type: none"> <li>- Black liquid similar to engine oil flowing from the turbocharger or the exhaust pipe.</li> <li>- Wet or dark fluid around the right side of the engine at the exhaust manifold</li> </ul>	Prolonged engine operation at a low load prevents the temperature from reaching its required value for the complete combustion of all the injected fuel.
Polishing cylinder	<ul style="list-style-type: none"> <li>- Increasing oil consumption</li> <li>- Power loss</li> </ul>	Local mechanical friction is probably due to carbon deposits around the rings caused by poor combustion from running the engine at a low load.
Glazing cylinder	<ul style="list-style-type: none"> <li>- Increasing oil consumption</li> <li>- Power loss</li> <li>- Engine smoke</li> </ul>	<ul style="list-style-type: none"> <li>- Engine cold start</li> <li>- Highly additive oil (extended oil change interval)</li> <li>- Underloaded operating condition</li> </ul>
Effects	<ul style="list-style-type: none"> <li>- Cost: The excessive occurrence of these phenomena reduces the remaining life of the engine and its main components by several years. These phenomena also increase fuel consumption and, consequently, costs.</li> <li>- Pollution: increases engine smoke and greenhouse gases.</li> <li>- Power: reduction of the maximum power produced by the engine compared to its nominal power.</li> <li>- Maintenance: a fixed-speed engine experiencing these problems requires more frequent maintenance than an engine operating with an adequate load.</li> </ul>	

To the best of the author's knowledge, experimental or research studies have yet to be done on the detection of underperformance of a fixed-speed diesel–electric generator based on exhaust gas emissions or attempted to address this issue when running under a low load in isolated communities during an extended period. However, the solutions being discussed today to address the issue of underperformance [16–22] may be an attractive approach for these communities. Still, they cannot be implemented shortly due to their outdated infrastructure and lack of access to clean fuels at these locations. Therefore, this study addresses the issue of preventing diesel generator underperformance by investigating diesel engine emissions and fuel consumption under three different load levels (i.e., very low, low, and regular). The paper contains six sections. After the introduction, Section 2 presents the

case of remote communities' electrification in northern Canada and the technical challenges affecting diesel–electric generators. Section 3, entitled Experimental Apparatus, presents the equipment used in the experiments, followed by Section 4 “Methodology”, which describes the methodology and applied tools. Section 5, Results and Discussion, gives the results obtained and the analysis performed. Finally, Section 6, Conclusion, synthesizes this work's findings and gives a perspective for future work.

## 2. Case of Remote Communities in Northern Canada

Remote communities in Canada, where most of the population is indigenous, rely on diesel fuel for heating and energy generation [23–27]. More precisely, to be self-sufficient in electrical energy, 79% of these remote communities favored fossil fuel generators, mainly diesel [28,29], as shown in Figure 1, due to their reliability and familiarity of the local utilities with the technology. We analyzed 213 remote Canadian communities for diesel use for electricity generation. Most diesel–electric generators in these isolated communities are oversized to meet peak demand. As a result, they can be five times greater than the average electrical load [5,30,31]. In addition, these generators typically are fixed-speed and run mostly at low loads (Table 2), leading to higher oil consumption and, consequently, a more significant deposit of carbonized oil or oil residue in the engine and its suction and exhaust system [32].

**Table 2.** Load levels as a percentage of rated power.

Power Percentage	Load Level
0–25%	Very low load
26–39%	Low load
40–80%	Regular load
81–90%	High load
91–100%	Very high load

The appearance and persistence of residue have a detrimental effect on the engine's lifespan and functioning behavior. Consequently, the number of maintenance activities tends to rise [33–35]. Additionally, an engine running in low-load mode cools down, which results in only partial fuel combustion and can produce white smoke with significant hydrocarbon emissions [36–38]. Furthermore, the proportion of incomplete combustion in the oil increases due to the low fuel temperature. Due to these issues, the oil leaks and is released through the exhaust valves because the piston rings, the piston itself, and the cylinder do not dilate enough to ensure a reliable seal. This indicates that the quality and characteristics of the lubricant are diminished as the diesel oil enters the crankcase [39]. One technique to address this issue and eliminate these deposits is to increase the engine speed until the operating temperature is attained. In the industry sector, especially in the USA, using a load bank is a standard technique to lessen these adverse effects [40]. On the other hand, combining small, new fixed-speed diesel–electric generators whose combined power energy output is equivalent to a single large, fixed diesel–electric generator can prevent the large engine from functioning under a low load [41].

In this study, we compare a diesel generator's exhaust emissions, exhaust temperature, and fuel consumption under two conditions: in the first scenario, the diesel generator will be subjected to low loads for a brief period (15 min) before being subjected to a load greater than 40%; while in the second scenario, the diesel generator will be subjected to low loads for a lengthy period (up to 2 h of operation) before being subjected to a load greater than 40% again. The final objective is to analyze the impact of short-term low-load operation versus long-term low-load operation on engine combustion and fuel consumption and to see if there is a possibility of preventing the deterioration of diesel engine efficiency from the results obtained.

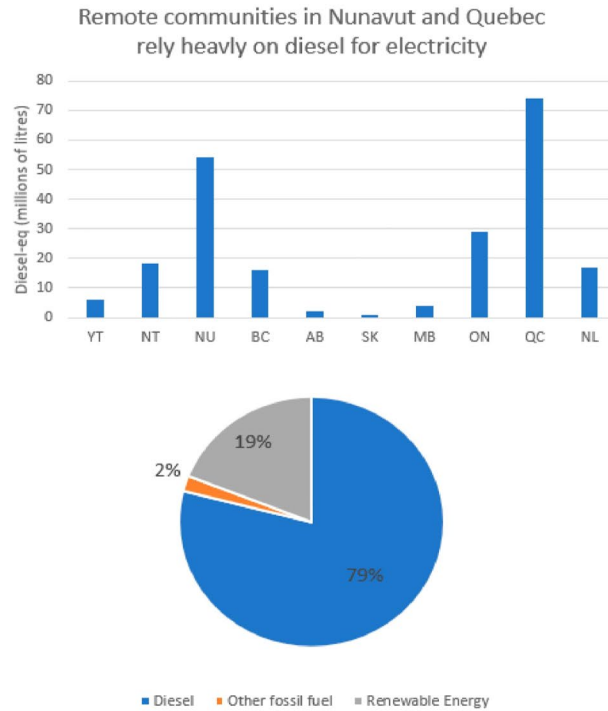


**Figure 1.** Remote communities in Canada, mainly Nunavut and Quebec, rely on diesel fuel for heating and electricity generation [42].

### 3. Experimental Apparatus

This study used an 8.8 L heavy-duty fuel compression ignition engine to drive a 300 kW alternator for the experiments. The engine has an efficiency of 36%. The test bench components and an overview of the layout are shown in Figures 2 and 3. The engine features advanced combustion emission reduction technology (ACERT), which integrates air and fuel controls to comply with the Environmental Protection Agency (EPA) 2004 requirements. Instead of using the Exhaust Gas Recirculation (EGR) technology, improved air management employs a series of turbochargers to push cool, clean air into the combustion chamber. Variable valve actuation, which complements the camshaft actuation, is also used by the engine to control airflow. The emissions are further decreased using a diesel oxidation catalyst. As the electrical frequency of the network grid is 60 Hz, the engine's speed was fixed at 1800 rpm throughout all the tests.

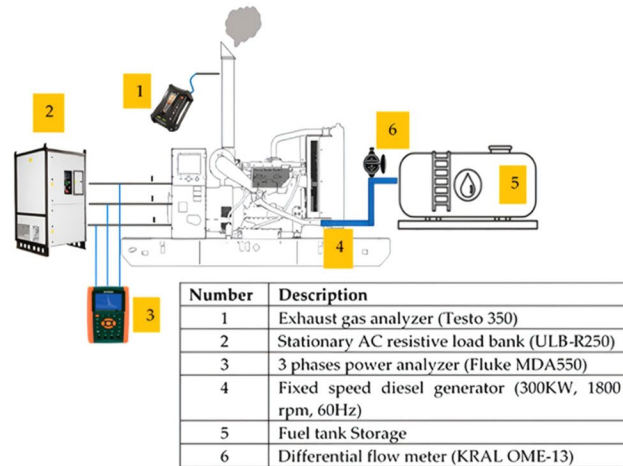


Figure 2. Schematic representation of the study's experimental design.



1	Load bank
2	Alternator
3	Flowmeter
4	Storage tank

Figure 3. Illustration of the test bench inside the insulated container installed in northern Quebec.

The engine specifications are presented in Table 3, while the generator specifications are in Table 4.

Table 3. Engine specifications.

Engine Type	Inline Six Cylinders, C9
Bore	112.0 mm
Stroke	149.1 mm
Displacement	8.8 L
Compression Ratio	16.1:1
Aspiration	Air to air aftercooled
Fuel system	Hydraulic electronic unit injection
Governor type	Adem A4

**Table 4.** Electrical generator specifications.

Standby Rating	300 ekW
Alternator design	Brushless single bearing, 4-pole
Stator	2/3 Pitch
No. of Leads	12
Voltage	208 V
Frequency	60 Hz
Voltage regulation, steady state +/-	≤0.5%

A fuel flow meter was mounted on the engine test bench to record the diesel fuel rate based on the differential measurement method. The feed line's flow rate and the consumer's return line are measured directly. The consumption formula is, therefore, the incoming minus the return flow. We used a KRAL flowmeter (OME-013 model) with a precision rate of  $\pm 0.1\%$  of the measurement value.

A flue gas analyzer (Testo 350 model) was used to measure the temperature and the exhaust gas emissions output. This flue gas analyzer has been specifically designed for industrial emission measurements such as diesel engines, gas turbines, and thermal processes. This analyzer is equipped with an analysis box that can be operated with up to 6 gas sensors such as sulfur dioxide (SO<sub>2</sub>), carbon dioxide (CO<sub>2</sub>), oxides of nitrogen (NO<sub>x</sub>), oxygen (O<sub>2</sub>), carbon monoxide (CO), and sulfur (S). Table 5 below shows the accuracy for the different gases according to the manufacturer.

**Table 5.** Accuracy rates for industrial emission measurements with the Testo 350 [43].

Flue Gas	Measuring Range	Accuracy	Resolution
CO <sub>2</sub>	0 to CO <sub>2</sub> max	calculated from O <sub>2</sub> $\pm 0.2$ Vol.%	0.01 Vol.%
O <sub>2</sub>	0 to +25 Vol.%	$\pm 0.8\%$ of fsv (0 to +25 Vol.%)	0.01 Vol.% (0 to +25 Vol.%)
CO	0 to +10,000 ppm	$\pm 5\%$ of mv (+200 to +2000 ppm) $\pm 10\%$ of mv (+2001 to +10,000 ppm) $\pm 10$ ppm (0 to +199 ppm)	1 ppm (0 to +10,000 ppm)
NO	0 to +4000 ppm	$\pm 5\%$ of mv (+100 to +1999 ppm) $\pm 10\%$ of mv (+2000 to +4000 ppm) $\pm 5$ ppm (0 to +99 ppm)	1 ppm (0 to +4000 ppm)
NOX	0 to +500 ppm	$\pm 5\%$ of mv (+100 to +2000 ppm) $\pm 10\%$ of mv (+2001 to +5000 ppm) $\pm 5$ ppm (0 to +99 ppm)	1 ppm (0 to +5000 ppm)
SOX	0 to +5000 ppm	$\pm 5\%$ of mv (+100 to +2000 ppm) $\pm 10\%$ of mv (+2001 to +5000 ppm) $\pm 5$ ppm (0 to +99 ppm)	1 ppm (0 to +5000 ppm)

#### 4. Methodology

The tests were conducted at an engine speed of 1800 rev/min. The fuel used during the tests was ultra-low sulfur diesel fuel (ULSD) for off-road engines (locomotive and vessel diesel engines) containing 15 ppm sulfur, compliant with the current standard for all engine diesel fuel defined by Environment Canada [44]. The loads were varied from 0 to 156 kW, which represents 0–52% of the maximum capacity of the generator, to recreate the electrical charge profile in an isolated microgrid in northern Quebec (Figure 4). All the tests were performed under an ambient temperature of 21 °C. The readings at each load were taken after the engine reached the steady-state condition. The following experimental parameters were determined.

1. Exhaust emission characteristics include exhaust gas temperature,  $\text{SO}_2$ ,  $\text{CO}_2$ ,  $\text{NO}_x$ ,  $\text{O}_2$ ,  $\text{CO}$ , and  $\text{S}$ .
2. The effect of Brake-Specific Fuel Consumption (BSFC)

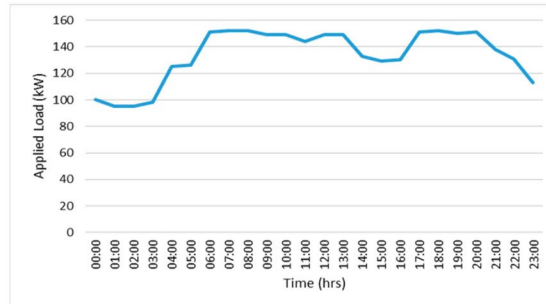


Figure 4. The remote community electrical load profile at Baie-James, Canada.

These readings were repeated three times for the very low load (0–25%), low load (26–39%), and regular load (40–52%). The tests were according to ISO 3046–1:2002 standard, including correcting the load power and fuel consumption findings to standard conditions [45].

## 5. Results and Discussion

### 5.1. Engine Performance: Brake Specific Fuel Consumption (BSFC)

Figure 5 depicts the BSFC at different loads. The analysis shows that the variation in fuel consumption as a function of the load varies instantaneously when switching from a low to a high load and vice versa, and this for both regimes: (i) normal performance regime where the engine has been subjected to a low load for a very short period (15 min), and (ii) underperformance regime where the engine has been subjected to a low load for an extended period (up to 2 h). However, an increase in fuel consumption was observed after 1.5 h of operation under loads of 4 to 35% before it was reduced and returned to normal for the last 30 min under loads ranging from 40 to 52%. For both regimes, there was no noticeable delay in the consumption curve. Moreover, regardless of the load value, the BSFC (in gallons per kWh produced) declines as the engine load increases. Higher fuel consumption is necessary to achieve the desired power output at a lower speed due to the lower pressure in the cylinders leading to lower volumetric efficiency. Therefore, BSFC decreases as engine speed increases and total energy utilization increases.

Additionally, the findings suggest that the BSFC decreases with engine load. The total energy released increases with engine load, and the proportion of output power rises because the friction loss is nearly identical [46,47]. Based on the BSFC results, fuel consumption might be viewed as a sign of low or high load operating rather than a reliable indicator of underperformance. This can be explained by the fact that the underperformance based on BSFC data is determined by the operation period (short or long time) under a low load. In this case, the operator must combine time and fuel consumption to determine if the engine performs below par. According to Caterpillar [33], the time limit for low load operation (0 to 30 percent) is fixed at 30 min.

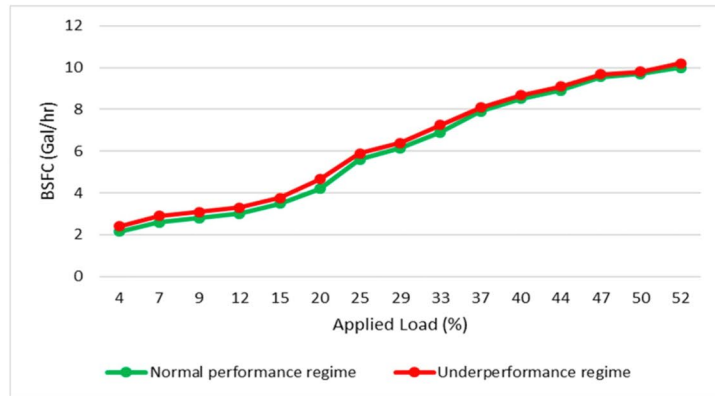


**Figure 5.** Break specific fuel consumption of the C9 fixed-speed diesel generator according to the applied loads under two scenarios.

#### 5.2. Exhaust Gas Temperature

The variation of exhaust gas temperature for different load conditions is presented in Figure 6. One can see that the exhaust gas temperature increases with the load. This occurs because more fuel is burned in the cylinder when the engine load increases, raising the cylinder temperature [48]. In addition, the exhaust gas temperature is highest when the engine runs at its highest speed. However, exhaust gas temperatures were found to be slightly higher for loads between 4 and 33% for extended periods under low loads (underperformance regime). Above 35%, the temperature stayed at the same level as when the engine was run briefly at a low load (normal performance regime). This could be because the fuel/air ratio in the cylinders is no longer operating as efficiently, which leads to poor combustion and a variation in exhaust gas temperatures.

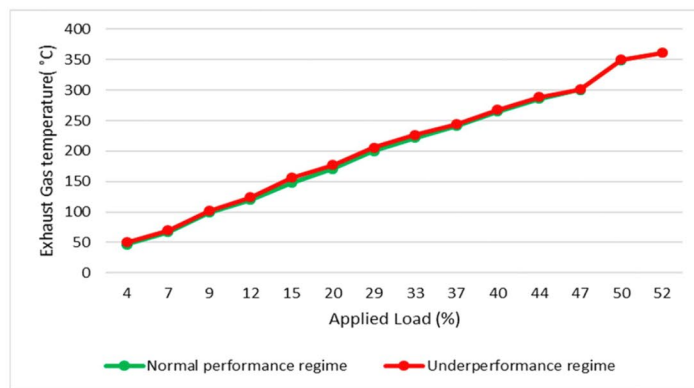


**Figure 6.** Exhaust gas temperature vs. load.

According to this graph, the variation of exhaust gas temperature as a function of the applied load can indicate underperformance. For example, at a very low load and low load (0–39%), the temperature does not exceed 250 °C for both regimes, while at a regular load (42–52%), the temperature reaches up to 360 °C. Furthermore, the exhaust gas temperature is linear versus the applied load. Although exhaust temperature increases with diesel engine load, we noticed during the experimental test that the temperature stabilizes in less than 12 min for both scenarios when the applied load varies, which confirms that it is possible to use this measure as an underperformance sign if operation time is taken into consideration. For example, extended time (>30 min) under low loads ( $\leq 30\%$ ) with a recorded temperature below 250 °C can be considered a sign of underperformance. In comparison, a recorded temperature of 250 °C or less for a short period (10–15 min) can be discarded.

### 5.3. Sulfur Emissions (S)

Burning fossil fuels that include sulfur produces the most sulfur oxide ( $\text{SO}_x$ ) in the atmosphere. When sulfur combines with oxygen during combustion, sulfur dioxide is created ( $\text{SO}_2$ ). Figure 7 indicates the variation of the sulfur emission for the load. The sulfur level in the exhaust gas is higher when the generator runs in the extended mode under a light load (underperformance regime) before reaching the normal value when the load increases beyond 35%. Furthermore, sulfur seems to be the best indication for underperformance detection. The sulfur level stabilizes at low load (10 ppm), while at very low load (<25%), it varies between 18 ppm to 12 ppm. This occurs because at low loads and speeds, the heat inside the combustion chamber will be inadequate for the rapid oxidation of sulfur atoms. At medium and high loads, the temperature of the combustion chamber increases, and the oxidation of all molecules is also improved [49]. Therefore, part of the sulfur content is oxidized to form  $\text{SO}_2$ , while other parts form other compounds such as aromatics and PM. Therefore, sulfur concentrations are reduced in this range.

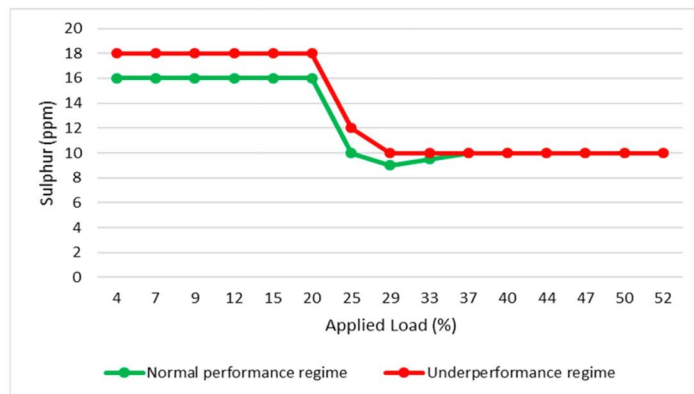


Figure 7. Variation of the S content in the exhaust gas according to the applied loads.

### 5.4. Sulfur Dioxide Emissions ( $\text{SO}_2$ )

Figure 8 indicates the variation of  $\text{SO}_2$  emission with the load. It is seen that the  $\text{SO}_2$  level stabilizes at 12–13 ppm when the load reaches 25–45% of the total available power, and the maximum percentage occurs at a very low load (12–15%) of up to 18 ppm. Based on the information presented in Figure 7, at a very low load (7–8%), the  $\text{SO}_2$  emission rate can create confusion in diesel engine underperformance detection, as its amount is identical to that of a low load and regular load (26–40%), making it a suboptimal indicator for diesel

engine underperformance. In addition, it was found at regular load (beyond 50%), the  $\text{SO}_2$  decreases further and reaches 10 ppm. Therefore, the explanation could be insufficient heat to evaporate the fumigation fuel effectively under a very low and low load [50].

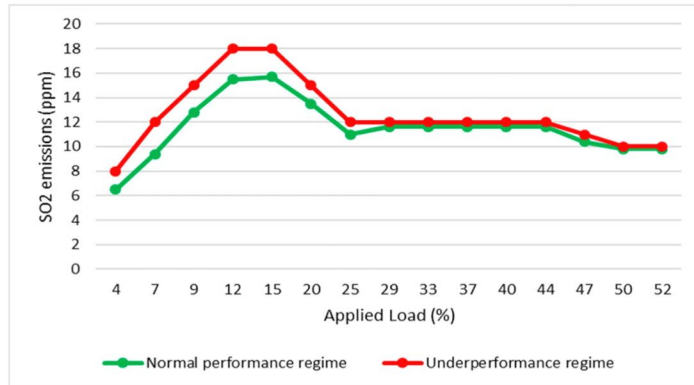


Figure 8. Variation of the  $\text{SO}_2$  rate according to the applied loads.

#### 5.5. Oxygen Emissions ( $\text{O}_2$ )

Figure 9 shows the variation of the oxygen rate emission with the load. In the recorded data, with an increase in load, the oxygen rate declines; for loads between 37% and 47%, the oxygen level nearly leveled out at 12 ppm, and this is for both tested regimes. In general, when the load increases, there is a greater need for fuel and oxygen in the combustion chamber, resulting in a linear decrease in oxygen emission. Therefore, oxygen rate, because of its linear behavior to the applied load, can be a good sign for the underperformance detection of a diesel engine. However, oxygen rate emission shows a decline at an underperformance regime before it returns to normal when the load reaches 40%.

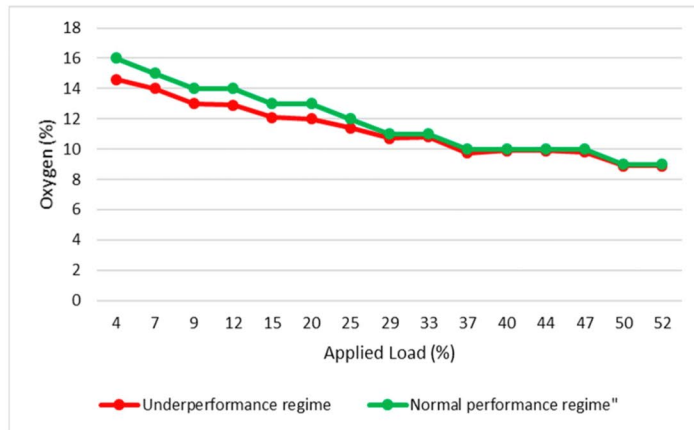
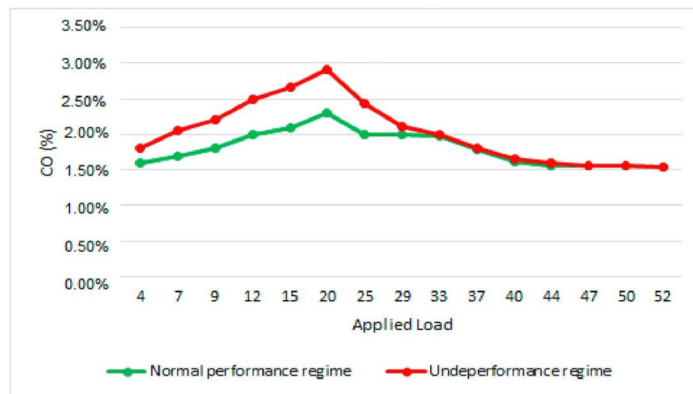


Figure 9. Variation of the  $\text{O}_2$  rate according to the applied loads.

### 5.6. Carbon Monoxide Emissions (CO)

Carbon monoxide, a colorless and odorless gas, appears in exhaust gases when combustion reactions are not fully completed due to low mixing or a shortage of oxygen [51]. Figure 10 indicates the variation of the carbon monoxide at different load conditions. It is found that the CO rate, despite its fluctuation, is significantly higher under a very low load and underperformance regime, and it tends to decrease to a stable level by increasing the load. Lower CO emission results from improved mixing and higher air ratios. Therefore, according to the obtained curve, CO can play a significant role as an underperformance detection method as it tends to stabilize around regular loads (37% and up).



**Figure 10.** Variation of the CO content in the exhaust gas according to the applied loads.

### 5.7. Nitrogen Oxide Emissions ( $NO_x$ )

The high temperature and pressure of the combustion chamber are the leading causes of nitrogen oxide formation, which are highly harmful environmental emissions. The generation of  $NO_x$  increases as temperature and air-to-fuel ratio increase. The various  $NO_x$  concentrations in the exhaust gas emission are depicted under various loads in Figure 11. As the load level increases, the temperature in the combustion chamber rises, leading to a proportional increase in  $NO_x$  emissions, which tends to level off in regular loads. Furthermore,  $NO_x$  tends to increase under an underperformance regime. Therefore,  $NO_x$  emissions can be considered an underperformance sign for diesel engines because of stabilizing in regular loads and its higher level at operation under prolonged time low load.

### 5.8. Carbon Dioxide Emissions ( $CO_2$ )

Carbon dioxide is released when the carbon atoms in the fuel are wholly oxidized during combustion. Although it is typically not subject to emission regulations and is not regarded as a dangerous gas, there is a solid requirement to minimize  $CO_2$  emissions because it is a greenhouse gas. The change in  $CO_2$  emissions with the load is shown in Figure 12. We notice a roughly linear increase in  $CO_2$  emissions with the load, and this is under both regimes. Additionally,  $CO_2$  emissions increase further when the generator runs in underperformance mode. This change was observed after one hour of prolonged operation under a light load (<30%). This finding suggests that  $CO_2$  level helps detect underperformance.

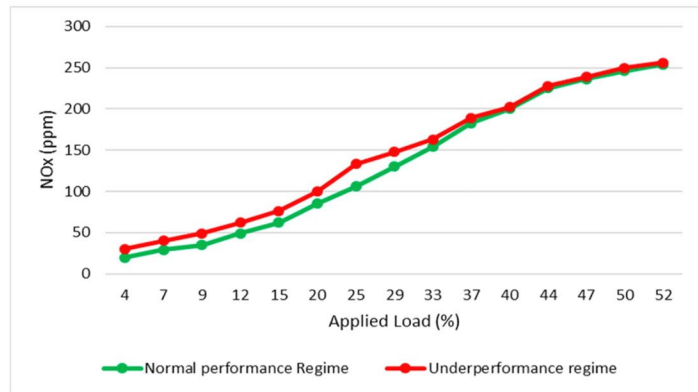


**Figure 11.** Variation of the NO<sub>x</sub> content in the exhaust gas according to the applied loads.

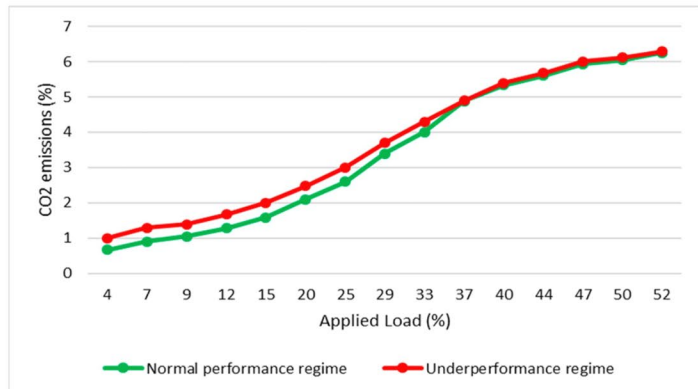


**Figure 12.** Variation of the CO<sub>2</sub> content in the exhaust gas according to the applied loads.

## 6. Conclusions

Remote communities are characterized by a strong dependence on imported fuels and by the high cost of energy. As a result, most of these locations supply their energy demand with diesel electrical generators either alone or in hybridization with renewable sources. However, most of these generators are oversized. In addition, because of the characteristics of their hosting power grids, they often tend to underperform for extended hours, which can have numerous negative long-term impacts on the generator.

This experimental study compares the outcomes of tests performed on a 300 kW fixed-speed diesel electric generator for the following charges during a transient regime of 15 min and another of an extended length of two hours:

1. Very low load.
2. Low load.
3. Medium load.

Analysis of the chemical composition, temperature, and fuel consumption of exhaust gases as a function of the applied load is performed to determine the transition time of emissions and identify pertinent signs when the generator is operating in underperformance mode. The test results led us to the following conclusions:

1. According to data analysis, it is found that under a very low load (0–25%), the exhaust gas temperature does not exceed 190 °C for an extended period of operation (up to 2 h), while under a 30% load, the temperature stabilizes at 220 °C; this is true for both regimes (extended period and not extended period). Therefore, it was concluded that the exhaust gas temperature could be used as an index of underperformance operation if prolonged operation time under low load is associated.
2. The BSFC showed an increase when the diesel–electric generator was subjected to a light load ( $\leq 30\%$ ) for a prolonged duration (up to 2 h) versus a short period (15 min). It recorded a 6.4 gallons/kWh consumption in underperformance operation at 30% of the applied load versus 6.14 gallons/kWh in normal operation. However, the BSFC returns to normal when the load attains 40% and registers 8.5 gallons/kWh. Based on the results obtained, the BSFC can be considered an underperformance index.
3. Analysis of gas emissions such as carbon monoxide and sulfur dioxide emissions have been discarded. This could be explained by the fact that some emission values are similar under low and normal loads.
4. Carbon dioxide emissions, nitrogen oxide emissions, and sulfur showed an increase in their levels when the generator was subjected to low load ( $\leq 30\%$ ) for a prolonged period (up to two hours) associated with underperformance operation. These gases tend to reach a normal emission level when the applied load increases to 40%. It was found that carbon dioxide emissions increase up to 0.5% under very-low and low loads (0–30%), nitrogen oxide emissions by up to 10 ppm, and sulfur by 2 ppm.
5. Finally, unlike all other gases, oxygen emissions decrease under very-low and low loads by up to 2% before reaching the normal level of emissions under a normal load (40% and above). This allows us to conclude that oxygen can be also considered an underperformance index.

**Author Contributions:** Conceptualization, M.G.; methodology, A.I. and M.I.; validation, M.I. and A.I.; investigation, M.G., M.I. and A.I.; resources, A.I.; writing—original draft preparation, M.G. and A.I.; writing—review and editing, M.I. and A.I.; supervision, M.I.; project administration, A.I. All authors have read and agreed to the published version of the manuscript.

**Funding:** This research received no external funding.

**Data Availability Statement:** Not applicable.

**Conflicts of Interest:** The authors declare that they have no known competing financial interest or personal relationship that could have appeared to influence the work reported in this paper.

## References

1. Abedin, M.J.; Imran, A.; Masjuki, H.H.; Kalam, M.A.; Shahir, S.A.; Varman, M.; Ruhul, A.M. An overview on comparative engine performance and emission characteristics of different techniques involved in diesel engine as dual-fuel engine operation. *Renew. Sustain. Energy Rev.* **2016**, *60*, 306–316. [\[CrossRef\]](#)
2. Buyukkaya, E. Effects of biodiesel on a DI diesel engine performance, emission and combustion characteristics. *Fuel* **2010**, *89*, 3099–3105. [\[CrossRef\]](#)
3. Ibrahim, H.; Issa, M.; Lepage, R.; Ilinca, A.; Perron, J. Supercharging of diesel engine with compressed air: Experimental investigation on greenhouse gases and performance for a hybrid wind–diesel system. *Smart Grid Renew. Energy* **2019**, *10*, 213. [\[CrossRef\]](#)
4. Wang, B.L.; Lee, C.W.; Reitz, R.D.; Miles, P.C.; Han, Z. A generalized renormalization group turbulence model and its application to a light-duty diesel engine operating in a low-temperature combustion regime. *Int. J. Engine Res.* **2013**, *14*, 279–292. [\[CrossRef\]](#)
5. Issa, M.; Rezkallah, M.; Ilinca, A.; Ibrahim, H. Grid integrated non-renewable based hybrid systems: Control strategies, optimization, and modeling. In *Hybrid Technologies for Power Generation*; Academic Press: Cambridge, MA, USA; Elsevier: Amsterdam, The Netherlands, 2022; pp. 101–135.

6. Issa, M.; Ibrahim, H.; Ilinca, A.; Hayyani, M.Y. A review and economic analysis of different emission reduction techniques for marine diesel engines. *Open J. Mar. Sci.* **2019**, *9*, 148. [CrossRef]
7. Issa, M.; Ilinca, A.; Martini, F. Ship Energy Efficiency and Maritime Sector Initiatives to Reduce Carbon Emissions. *Energies* **2022**, *15*, 7910. [CrossRef]
8. Fayad, A.; Ibrahim, H.; Ilinca, A.; Sattarpanah Karganroudi, S.; Issa, M. Energy Recovering Using Regenerative Braking in Diesel–Electric Passenger Trains: Economical and Technical Analysis of Fuel Savings and GHG Emission Reductions. *Energies* **2021**, *15*, 37. [CrossRef]
9. Barbosa, R.; Issa, M.; Silva, S.; Ilinca, A. Variable Speed Diesel Electric Generators: Technologies, Benefits, Limitations, Impact on Greenhouse Gases Emissions and Fuel Efficiency. *J. Energy Power Technol.* **2022**, *4*, 3. [CrossRef]
10. James, C.J. Analysis of Parasitic Losses in Heavy Duty Diesel Engines. Doctoral Dissertation, Massachusetts Institute of Technology, Cambridge, MA, USA, 2012.
11. Yang, B.; Xi, C.; Wei, X.; Zeng, K.; Lai, M.C. Parametric investigation of natural gas port injection and diesel pilot injection on the combustion and emissions of a turbocharged common rail dual-fuel engine at low load. *Appl. Energy* **2015**, *143*, 130–137. [CrossRef]
12. Duan, X.; Liu, Y.; Liu, J.; Lai, M.C.; Jansons, M.; Guo, G.; Zhang, S.; Tang, Q. Experimental and numerical investigation of the effects of low-pressure, high-pressure and internal EGR configurations on the performance, combustion and emission characteristics in a hydrogen-enriched heavy-duty lean-burn natural gas SI engine. *Energy Convers. Manag.* **2019**, *195*, 1319–1333. [CrossRef]
13. Yousefi, A.; Guo, H.; Birouk, M. An experimental and numerical study on diesel injection split of a natural gas/diesel dual-fuel engine at a low engine load. *Fuel* **2018**, *212*, 332–346. [CrossRef]
14. Wei, L.; Geng, P. A review on natural gas/diesel dual fuel combustion, emissions and performance. *Fuel Process. Technol.* **2016**, *142*, 264–278. [CrossRef]
15. Rao, X.; Sheng, C.; Guo, Z.; Yuan, C. A review of online condition monitoring and maintenance strategy for cylinder liner-piston rings of diesel engines. *Mech. Syst. Signal Process.* **2022**, *165*, 108385. [CrossRef]
16. Bao, J.; Wang, H.; Wang, R.; Wang, Q.; Di, L.; Shi, C. Comparative Experimental Study on Macroscopic Spray Characteristics of Various Oxygenated Diesel Fuels. *Energy Sci. Eng.* **2023**. [CrossRef]
17. Shi, C.; Chai, S.; Di, L.; Ji, C.; Ge, Y.; Wang, H. Combined experimental-numerical analysis of hydrogen as a combustion enhancer applied to Wankel engine. *Energy* **2023**, *263*, 125896. [CrossRef]
18. Abbas, T.; Issa, M.; Ilinca, A. Biomass cogeneration technologies: A review. *J. Sustain. Bioenergy Syst.* **2020**, *10*, 1–15. [CrossRef]
19. Issa, M.; Fiset, J.; Mobarra, M.; Ibrahim, H.; Ilinca, A. Optimizing the performance of a 500 kW Diesel Generator: Impact of the Eo-Synchro concept on fuel consumption and greenhouse gases. *Power Eng.* **2018**, *23*, 22–31.
20. Bao, J.; Qu, P.; Wang, H.; Zhou, C.; Zhang, L.; Shi, C. Implementation of various bowl designs in an HPDI natural gas engine focused on performance and pollutant emissions. *Chemosphere* **2022**, *303*, 135275. [CrossRef]
21. Chen, Y.; Feng, L.; Mansir, I.B.; Taghavi, M.; Sharma, K. A new coupled energy system consisting of fuel cell, solar thermal collector, and organic Rankine cycle: generation and storing of electrical energy. *Sustain. Cities Soc.* **2022**, *81*, 103824. [CrossRef]
22. Pereyra-Mariñez, C.; Andrickson-Mora, J.; Ocaña-Guevera, V.S.; Santos García, F.; Vallejo Diaz, A. Energy Supply Systems Predicting Model for the Integration of Long-Term Energy Planning Variables with Sustainable Livelihoods Approach in Remote Communities. *Energies* **2023**, *16*, 3143. [CrossRef]
23. Issa, M. Optimisation Opérationnelle, Écologique et Énergétique des Groupes Électrogènes Diesel. Ph.D. Thesis, Université du Québec à Rimouski, Rimouski, QC, Canada, 2020.
24. Issa, M.; Ibrahim, H.; Lepage, R.; Ilinca, A. A review and comparison on recent optimization methodologies for diesel engines and diesel power generators. *J. Power Energy Eng.* **2019**, *7*, 31. [CrossRef]
25. Rehman, S. Hybrid power systems—Sizes, efficiencies, and economics. *Energy Explor. Exploit.* **2021**, *39*, 3–43. [CrossRef]
26. Arriaga, M.; Cañizares, C.A.; Kazerani, M. Northern lights: Access to electricity in Canada’s northern and remote communities. *IEEE Power Energy Mag.* **2014**, *12*, 50–59. [CrossRef]
27. Froese, S.; Kunz, N.C.; Ramana, M. Too small to be viable? The potential market for small modular reactors in mining and remote communities in Canada. *Energy Policy* **2020**, *144*, 111587. [CrossRef]
28. Katiraei, F.; Abbey, C. Diesel plant sizing and performance analysis of a remote wind-diesel microgrid. In Proceedings of the 2007 IEEE Power Engineering Society General Meeting, Tampa, FL, USA, 24–28 June 2007; pp. 1–8.
29. McFarlan, A. Techno-economic assessment of pathways for electricity generation in northern remote communities in Canada using methanol and dimethyl ether to replace diesel. *Renew. Sustain. Energy Rev.* **2018**, *90*, 863–876. [CrossRef]
30. Mobarra, M.; Rezkallah, M.; Ilinca, A. Variable Speed Diesel Generators: Performance and Characteristic Comparison. *Energies* **2022**, *15*, 592. [CrossRef]
31. Sedaghat, B.; Jalilvand, A.; Noroozian, R. Design of a multilevel control strategy for integration of stand-alone wind/diesel system. *Int. J. Electr. Power Energy Syst.* **2012**, *35*, 123–137. [CrossRef]
32. Issa, M.; Ibrahim, H.; Hosni, H.; Ilinca, A.; Rezkallah, M. Effects of low charge and environmental conditions on diesel generators operation. *Eng* **2020**, *1*, 137–152. [CrossRef]
33. Jabeck, B. The Impact of Generator Set Underloading (Caterpillar). Available online: [https://www.cat.com/en\\_US/by-industry/electric-power/Articles/White-papers/the-impact-of-generator-set-underloading.html](https://www.cat.com/en_US/by-industry/electric-power/Articles/White-papers/the-impact-of-generator-set-underloading.html) (accessed on 1 February 2022).

34. Tufte, E.D. Impacts of Low Load Operation of Modern Four-Stroke Diesel Engines in Generator Configuration. Master's Dissertation, Institutt for Marin Teknikk, Trondheim, Norway, 2014.
35. Hamilton, J.; Negnevitsky, M.; Wang, X. Low load diesel perceptions and practices within remote area power systems. In Proceedings of the 2015 International Symposium on Smart Electric Distribution Systems and Technologies (EDST), Vienna, Austria, 8–11 September 2015; pp. 121–126.
36. Mustayen, A.; Rasul, M.; Wang, X.; Negnevitsky, M.; Hamilton, J. Remote areas and islands power generation: A review on diesel engine performance and emission improvement techniques. *Energy Convers. Manag.* **2022**, *260*, 115614. [CrossRef]
37. Mustayen, A.; Wang, X.; Rasul, M.; Hamilton, J.; Negnevitsky, M. Theoretical investigation of combustion and performance analysis of diesel engine under low load conditions. *IOP Conf. Ser. Earth Environ. Sci.* **2021**, *838*, 012013. [CrossRef]
38. Saiyisitpanich, P.; Lu, M.; Keener, T.C.; Liang, F.; Khang, S.-J. The effect of diesel fuel sulfur content on particulate matter emissions for a nonroad diesel generator. *J. Air Waste Manag. Assoc.* **2005**, *55*, 993–998. [CrossRef] [PubMed]
39. Penny, M.A.; Jacobs, T.J. Efficiency improvements with low heat rejection concepts applied to diesel low temperature combustion. *Int. J. Engine Res.* **2016**, *17*, 631–645. [CrossRef]
40. German-Galkin, S.; Tarnapowicz, D.; Matuszak, Z.; Jaskiewicz, M. Optimization to limit the effects of underloaded generator sets in stand-alone hybrid ship grids. *Energies* **2020**, *13*, 708. [CrossRef]
41. Ayodele, T.; Ogunjuyigbe, A.; Akinola, O. n-split generator model: An approach to reducing fuel consumption, LCC, CO<sub>2</sub> emission and dump energy in a captive power environment. *Sustain. Prod. Consum.* **2017**, *12*, 193–205. [CrossRef]
42. Ferrier, L.; Ibrahim, H.; Issa, M.; Ilinca, A. State of the Art of Telecommunication Systems in Isolated and Constrained Areas. *Sensors* **2021**, *21*, 3073. [CrossRef] [PubMed]
43. Testo. Testo 350—Portable Emission Analyzer. Available online: <https://www.testo.com/en-US/testo-350/p/0632-3510> (accessed on 1 February 2023).
44. Government of Canada. Consultations on Potential Amendments to Sulphur in Diesel Fuel Regulations—Compendium of Stakeholder Comments. 2006. Available online: <https://www.canada.ca/en/environment-climate-change/services/canadian-environmental-protection-act-registry/sulphur-diesel-fuel-regulations-consultations.html> (accessed on 19 October 2022).
45. ISO 3046-1:2002; Reciprocating Internal Combustion Engines—Performance—Part 1: Declarations of Power, Fuel and Lubricating Oil Consumptions, and Test Methods—Additional Requirements for Engines for General Use. International Organization for Standardization: Geneva, Switzerland, 2002. Available online: <https://www.iso.org/obp/ui/#iso:std:iso:3046-1:ed-5:v:1:en> (accessed on 19 October 2022).
46. Fahd, M.E.A.; Wenming, Y.; Lee, P.; Chou, S.; Yap, C.R. Experimental investigation of the performance and emission characteristics of direct injection diesel engine by water emulsion diesel under varying engine load condition. *Appl. Energy* **2013**, *102*, 1042–1049. [CrossRef]
47. Ghobadian, B.; Yusaf, T.; Najafi, G.; Khatamifar, M. Diesterol: An environment-friendly IC engine fuel. *Renew. Energy* **2009**, *34*, 335–342.
48. Agarwal, A.K.; Srivastava, D.K.; Dhar, A.; Maurya, R.K.; Shukla, P.C.; Singh, A.P. Effect of fuel injection timing and pressure on combustion, emissions and performance characteristics of a single cylinder diesel engine. *Fuel* **2013**, *111*, 374–383. [CrossRef]
49. Liu, Y.; Peng, L.; Ngo, H.H.; Guo, W.; Wang, D.; Pan, Y.; Sun, J.; Ni, B.J. Evaluation of nitrous oxide emission from sulfide-and sulfur-based autotrophic denitrification processes. *Environ. Sci. Technol.* **2016**, *50*, 9407–9415. [CrossRef]
50. Jha, P.R.; Partridge, K.R.; Krishnan, S.R.; Srinivasan, K.K. Impact of low reactivity fuel type on low load combustion, emissions, and cyclic variations of diesel-ignited dual fuel combustion. *Int. J. Engine Res.* **2023**, *24*, 42–63. [CrossRef]
51. Li, T.; Suzuki, M.; Ogawa, H. Effect of two-stage injection on unburned hydrocarbon and carbon monoxide emissions in smokeless low-temperature diesel combustion with ultra-high exhaust gas recirculation. *Int. J. Engine Res.* **2010**, *11*, 345–354. [CrossRef]

**Disclaimer/Publisher's Note:** The statements, opinions and data contained in all publications are solely those of the individual author(s) and contributor(s) and not of MDPI and/or the editor(s). MDPI and/or the editor(s) disclaim responsibility for any injury to people or property resulting from any ideas, methods, instructions or products referred to in the content.



## **CHAPTER 3: COMPARATIVE ANALYSIS OF ANN MODELS IN INDUSTRIAL CONTROL SYSTEMS**

Artificial neural networks (ANNs) are a sub-field of machine learning modeled after the composition and operation of biological neural networks. Due to their versatility and adaptability, artificial neural networks (ANNs) are practical computational tools characterized by non-linear operations and capabilities that find practical applications across diverse domains, including industrial control systems, where precision and efficiency are paramount. This chapter explores various ANN models, delving into their strengths and limitations within industrial settings. The main objective is to assess and narrow down the existing architectures to the most optimal alternatives for our case study.

### **3.1 ANN JUSTIFICATION**

As a substitute for statistical forecasting methods like multiple regression, ANNs have gained popularity over the years. One of the main downsides of various regression models is the necessity of making several assumptions about the data, such as linearity, normality, homoscedasticity, and independence of errors. Without these assumptions, the model may not be valid, and the outcomes may not be trustworthy. Another drawback of the multiple regression model is multicollinearity. When two or more predictor variables are highly correlated, the regression model's ability to predict outcomes may be undermined, resulting in unstable and unreliable estimates of the regression coefficients (Shams et al., 2021). In comparison, ANNs are not prone to any limitations and require fewer assumptions, eliminating the need to choose a model in advance. Some of the benefits of ANNs over statistical forecasting models like multiple regression include but are not limited to:

- Capacity to manage non-linear relationships: ANNs can model non-linear relationships between input and output variables, while multiple regression can only handle linear correlations.

- Data handling: ANNs are more adept at handling missing or noisy data than multiple regression models.
- High-dimensional data handling: While multiple regression may become cumbersome with numerous input factors, ANNs can handle massive datasets with many input variables and can extract meaningful features from the data.
- Better generalization: ANNs perform better on unseen datasets because they have a higher generalization capacity than multiple regression.
- Stability and flexibility: A neural network's stability and flexibility allow it to retain previously learned information while accepting new inputs without losing the previously acquired knowledge.

Overall, ANNs can extract patterns and discover trends that are very difficult for people and computers to recognize because of their exceptional capacity to draw findings from complicated data. However, there are some inherent drawbacks of ANNs that researchers are trying to address. One of these difficulties is that the accuracy of the results of the neural networks depends on the size of the training set, and the future performance of the network cannot be predicted (Alexander, 2020).

## **3.2 ANN CLASSIFICATION AND COMPARISON**

ANN models can generally be classified based on various factors, such as architecture, learning algorithms, and application. These elements significantly contribute to ANN functionalities in different problems investigated in this section to determine the most suitable one for our problem.

### **3.2.1 Learning Algorithm**

The classification of ANN models based on learning paradigms refers to how an artificial neural network learns from its data input. Four main learning algorithms include fixed weight, supervised learning, unsupervised learning, and reinforcement learning.

1. Fixed weight: One of the ways to train Artificial neural networks (ANNs) is through fixed-weight training algorithms, in which the network's weights are predetermined and maintained during the training process. This contrasts with other training methods, which update the weights depending on the error between the intended output and the forecasted output during training. Fixed-weight training applications are limited to pre-training and information optimization, simple feature extractions, and compression. As our problem in this research is related to function approximation, the ability of an ANN to adjust its weights during training is crucial for effectively capturing and representing complex relationships within data, which makes it an unsuitable choice for our study.
2. Non-supervised training: In non-supervised training, ANN is trained without using labeled data, and its objective is to find patterns or structures in the data. Therefore, there is no optimum output to adjust the weights by comparing the network output with the error value. Instead, weights are updated only based on input pattern information. In non-supervised learning, the network is given a set of input data to find patterns or relationships between the data based on the clustering strategy without prior knowledge of what the clusters should look like. When the data is presented to the input layer, the learning algorithm operates based on a superior matching method, where the network connections are adjusted in a competition amongst the output layer nodes, and the node with the greatest value is chosen. Some applications of unsupervised learning include clustering, anomaly detection, association mining, and dimensionality reduction. Despite many unsupervised learning applications, determining the results' accuracy and the meaningfulness of the learnt models is difficult in the absence of labelled data. This phenomenon is often referred to as the "unsupervised learning paradox." (Alloghani et al., 2020). Choosing the right evaluation metrics is another challenge of this training algorithm, as the quality of the results varies on the particular job and application, and they do not properly represent how the model performed on a certain task. Furthermore, the selection of hyperparameters, such as the number of clusters or the size of the reduced

model, might affect how unsupervised learning methods perform. Due to this sensitivity, the settings may need to be carefully adjusted, which can take time and be costly in computing (Dike et al., 2018).

3. **Supervised training:** In supervised learning, the target variable is predicted based on the input data in a way that the associated outputs for each set of inputs are shown on the grid, and the weights are adjusted until the network output difference between the intended outputs and training outputs is within the permissible error range. The reason why this training algorithm is named “supervised” is because the algorithm is trained on a labeled data set. The objective of supervised learning is to develop a model that can correctly predict new, unforeseen data by training the data and then categorizing it by feeding it into input vectors that might or might not have previously been trained on the network. This characteristic of the supervised learning algorithm facilitates the neural network to learn a mapping from inputs to outputs, enabling it to make accurate predictions on new, unseen data (Alloghani et al., 2020). This makes this learning algorithm a suitable alternative for our research problem. The examples of ANN architectures using this learning method are Feedforward Neural Networks (FFNN), Multilayer Perceptron (MLP), Convolutional Neural Networks (CNN), and Recurrent Neural Networks (RNN).
4. **Reinforcement training:** In this training model, no training patterns exist, and the algorithm learns from trial and error by receiving rewards for good actions and penalties for bad ones. Therefore, the system’s performance is gradually enhanced over time by the algorithm learning to make choices in each environment (a state between supervised and unsupervised learning)(Alexander, 2020). Reinforcement learning can address various issues and has already shown outstanding achievements in several fields. However, it has several drawbacks, including the complexity of establishing the reward function and the computational demands of many algorithms. The topic of reinforcement learning is still developing and has a lot of space for study and advancement (Sutton & Barto, 2018).

### 3.2.2 ANN Architecture

Artificial Neural Network (ANN) models can be classified into two main categories based on the direction of information flow within the network: Feedforward Neural Networks (FFNN) and Recurrent Neural Networks (RNN)

#### 3.2.2.1 Feedforward Neural Network

In a feedforward neural network, information travels unidirectionally, passing from the input layer through one or more hidden layers before reaching the output layer. Models such as Single Layer Perceptron, as well as Multilayer Perceptron (MLP), Convolutional Neural Network (CNN), and Radial Basis Function Networks (RBFN) fall under the feedforward category. Single-layer feedforward neural network (SLP) models comprise an input and an output layer. Due to their linear nature, these models can only learn linear decision boundaries, making them less effective for tasks that demand capturing non-linear relationships in the data. Consequently, they find more practical use in binary classification problems, where the task involves classifying input patterns into one of two classes. The inherent simplicity of SLPs limits their capacity to handle more intricate patterns or relationships commonly found in complex real-world datasets (Hoang et al., 2021). On the other hand, Multi-layer FFNN models consist of at least one hidden layer of neurons between the input and output layers, which helps them model and approximate non-linear functions more effectively. MLPs exhibit versatility and find application in various function approximation problems, encompassing regression tasks, time series prediction, and intricate mapping challenges. This versatility is a crucial factor driving the adoption of this neural network model in numerous studies within the field of industrial control systems. Specifically, when addressing topics like diesel engine generator performance and exhaust emission prediction, MLPs prove to be valuable tools for their ability to handle complex relationships and provide accurate approximations (Fang et al., 2021; Fang et al., 2022; Ganesan et al., 2015; Shirneshan et al., 2022). Radial Basis Function neural networks (RBF) are another form of FFNN that have a wide range of machine learning applications, such as

pattern recognition, function approximation, and time-series prediction. In an RBF neural network, the hidden layer contains a set of radial basis functions that transform the input data into a high-dimensional space. The radial basis functions are mathematically expressed as a function of the Euclidean distance between the input vector and a set of center vectors. In general, clustering methods like K-means produce the center vectors. The radial basis functions are often Gaussian functions, meaning they peak at their centroid and decrease in amplitude as the distance from the centroid increases. The mathematical expression of the Gaussian function is given by:

$$\varphi(x) = \exp\left(\frac{-\|x-c\|^2}{2\sigma^2}\right) \quad (3.1)$$

Where  $x$  is the input vector,  $c$  is the center vector,  $\sigma$  is the width parameter, and  $\|\cdot\|$  represents the Euclidean distance.

The RBF network is typically trained in a supervised manner using a process called “training with centers.” In order to train the network, a collection of center vectors must be chosen from the input data. The difference between the network’s output and the target values for a given input is then minimized by adjusting the weights for each RBF function using a type of linear regression. This procedure can be repeated in an iterative manner by utilizing a training dataset consisting of input-output pairs until the network exhibits a satisfactory performance on a validation dataset. The selection of the RBF architecture in industrial control settings is usually because of a number of advantages compared to other network types such as its fast training and less complicated topology (Goga et al., 2023; Liao et al., 2023). The primary drawback of RBF networks in comparison to MLP lies in the challenge of selecting the optimal number of radial basis functions. If this number is not chosen carefully, there is a risk of the network becoming susceptible to overfitting. Convolutional Neural Networks (CNN) are another architecture of FFNN, which is mostly used for tasks involving visual data such as image classification, object detection, face detection, etc. However, as these specific applications are not directly aligned with the scope of our research problem, they are not explored further in our study.

### 3.2.2.2 Recurrent Neural Networks (RNN)

The second major categorization of neural networks is represented by Recurrent Neural Networks (RNN). In contrast to feedforward neural networks (FFNN), where data undergoes a one-time pass from input to output, RNNs feature looped connections that preserve information within the network. This inherent structure empowers RNNs to discern patterns in sequential data by retaining knowledge of past inputs. Consequently, RNNs prove advantageous in tasks where the temporal order of inputs holds significance, as seen in applications like Natural Language Processing (NLP), speech recognition, and time-series prediction. Notably, virtual assistants such as Siri and Cortana are examples of the practical application of this neural network architecture. While RNNs have many applications in sequential or time-series data, they are less commonly used for regression problems. One of the significant challenges attributed to RNNs is their vanishing gradient problem. This occurs when the gradient of loss function becomes very small, impeding the effective learning of long-term dependencies. As a result, RNNs may face difficulties in accurately capturing intricate patterns, particularly in regression problems. Training complexity of RNNs is another problem that arises when the dataset is fairly large, which makes this structure less practical for some regression problems (Hewamalage et al., 2021).

A comprehensive analysis of various neural network architectures reveals that Multilayer Perceptron (MLP) and Radial Basis Function (RBF) neural networks stand out as the predominant choices in numerous studies related to predicting diverse attributes in diesel engines. These attributes span from exhaust gas predictions to the overall performance of the engine, all of which proved that the implemented FFNNs were very effective prediction methods with minimal error (Ganesan et al., 2015; Hoang et al., 2021; Kshirsagar & Anand, 2017; Roy et al., 2014). The main rationale behind their selection for further exploration in the subsequent chapters of this research is the acknowledgment of the effectiveness demonstrated by these two architectures in prior studies.



## **CHAPTER 4: DESIGN AND IMPLEMENTATION OF ANN ALGORITHMS FOR DIESEL GENERATOR OPTIMIZATION**

### **4.1 INTRODUCTION**

The utilization of Artificial Neural Networks (ANNs) for function approximation tasks encompasses a wide range of applications, such as image processing, voice recognition, and control systems. Function approximation refers to the problem of finding a mathematical function that maps input variables into output variables, and it is particularly useful when the target function is challenging to model directly because of its complexity or non-linearity, making it unclear how inputs and outputs are related. We can predict future inputs and outputs by approximating the target function and control the network's behavior. In this study, to detect and prevent the underperformance of a diesel engine generator based on the selected operational parameters in Chapter 2, such as certain emission gases and operating temperature, we need a function that closely matches or approximates the operating load of the DEG.

### **4.2 NEURAL NETWORK ARCHITECTURE SELECTION**

After identifying the best input values for our neural network, the next crucial step is selecting the best architecture that suits our requirements to leverage its capabilities effectively. The neural network's structure typically hinges on factors such as the number of hidden layers, the activation functions utilized within each layer, and the number of neurons in each layer. These parameters heavily influence the neural network's performance, underscoring their critical significance. While specific parameters can be determined by the characteristics of the problem being investigated, other parameters require alternative methods such as trial and error. This research uses two of the most popular neural networks, MLP and RBF, commonly used for function approximation problems.

Figure 2 illustrates a series of steps for implementing the neural network. Upon acquiring the dataset, the initial step involves preprocessing, wherein the data is normalized.

Subsequently, the dataset is appropriately allocated among the train, test, and validation sets, ensuring an optimal neural network training ratio. After the primary simulation of the ANN model, we examine the changes in the structure of each network and their impact on the output to fine-tune the network's critical parameters.

When investigating the optimal structure for each network, the data allocation for the test, train, and validation dataset remains the same as determined in the previous stage. In this phase, critical areas of consideration include selecting the suitable training algorithm, choosing the ideal arrangement of hidden layers, configuring neurons within each layer, and specifying the number of required training iterations. The network's errors were then compared, and the lowest error was recorded. The same process is also done for the RBF network by fine-tuning the spread coefficient and the number of intermediate layer neurons to register the lowest obtained error. In the final stage, the lowest errors obtained from the previous stage are compared while considering factors such as the network's response time and complexity to determine the optimal model for our problem.

### **4.3 ANN MODELING**

Modeling an artificial neural network involves designing and training the network to predict outcomes based on input data. This typically involves selecting the appropriate architecture and parameters, feeding the network with relevant input data, defining the desired outputs, and training the network by iteratively adjusting the weights and biases of the network using techniques like backpropagation. This modeling process is discussed thoroughly in the following sections.

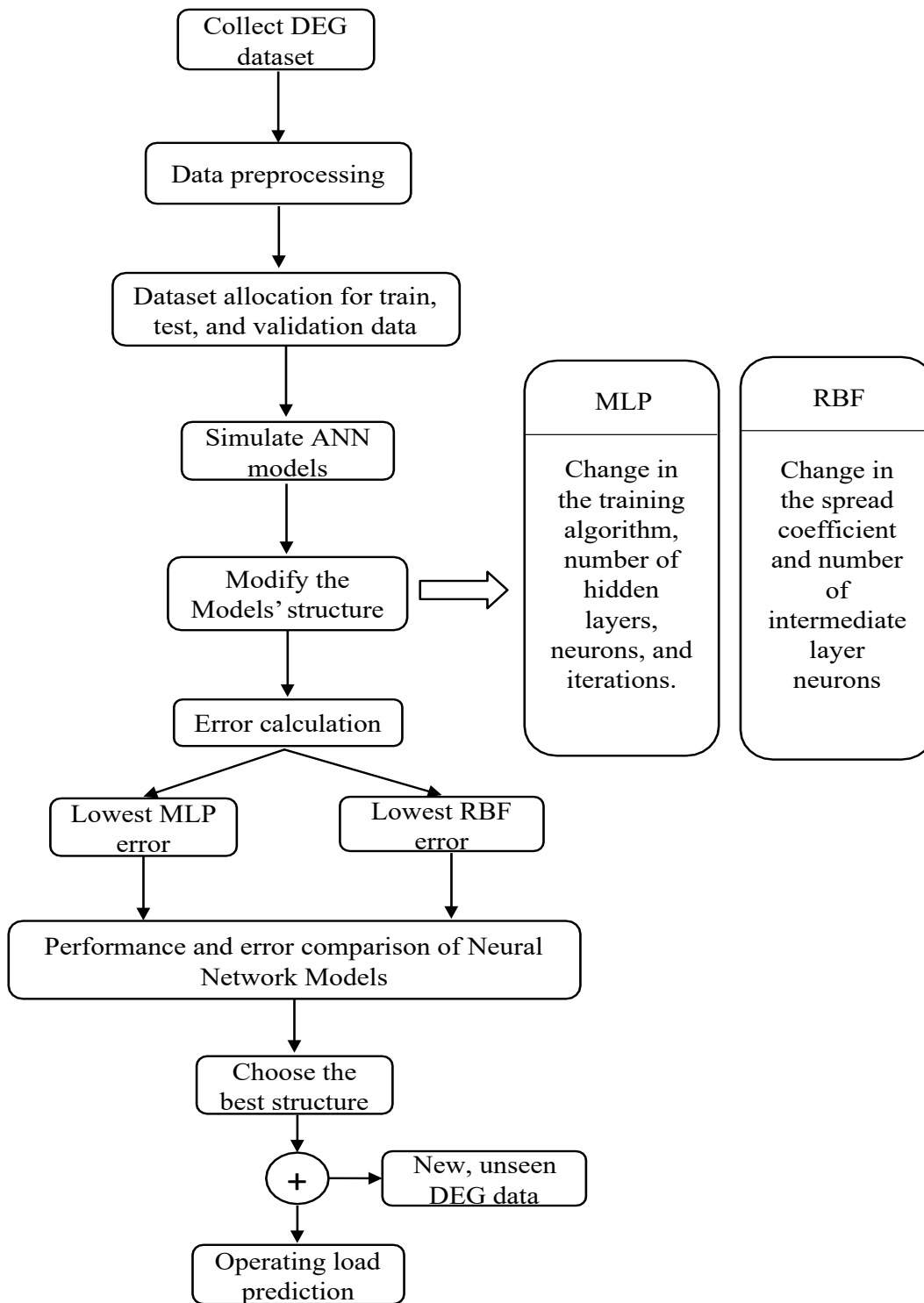


Figure 2 Neural Network Architecture selection procedure

### 4.3.1 Selection of input and output parameters

The choice of input variables significantly impacts the performance of an Artificial Neural Network (ANN) model. The quality and relevance of the input values can considerably affect the model's accuracy. The model's success may be compromised if the input data fails to capture the necessary information correlated with the target data. Out of all the measured data from the diesel engine generator in Chapter 2, the most pertinent ones were chosen for the input dataset of the ANN model to predict the diesel engine's operating load without overcomplicating our model. These input data include the exhaust gas temperature of the DEG, as well as certain emissions such as Sulfur (S), Carbon Monoxide (CO), Carbon dioxide (CO<sub>2</sub>), and Oxygen emission (O<sub>2</sub>). Therefore, the implemented FFNN includes five inputs and one output parameter, illustrated in Figure 3. This research uses MATLAB for every stage of model development, encompassing network training, testing, and validation.

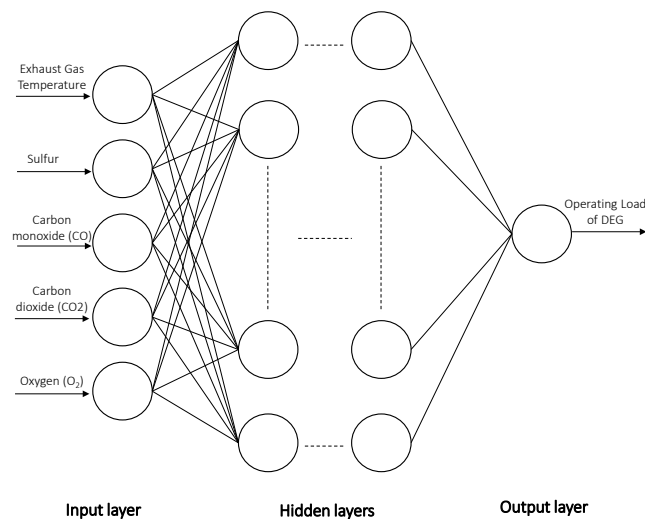


Figure 3 FFNN architecture used in this study

### 4.3.2 Data normalization

Data normalization is the process of scaling and converting the input data to a standardized format, allowing the ANN model to train more efficiently and precisely. To clarify further, during artificial neural network (ANN) training, inputs with higher values can potentially overshadow the influence of smaller ones. Therefore, to ensure that the model learns from all the characteristics equally, without bias toward any particular features, data normalization aims to ensure that each input feature has the same size, range, and distribution. This can improve an ANN's performance and speed, accuracy, and stability. One of the most common data normalization techniques is min-max normalization equation 4.1, which is a good choice when the distribution of the data is not Gaussian as it can avoid shifting the distribution of the data:

$$x_n = \frac{(x-x_{min})}{(x_{max}-x_{min})} \quad 4.1$$

### 4.3.3 Statistical assessment of output parameters

To make informed decisions regarding the artificial neural network (ANN) structure and the choice of training, testing, and validation datasets, it is crucial to establish the evaluation metrics that will assess the predictive performance of the suggested ANN model. Some commonly used evaluation metrics include Mean Squared Error (MSE) and Root Mean Squared Error (RMSE), which are standard methods for evaluating the performance of regression models and can be calculated using the equations below.

$$MSE = \frac{1}{n} \sum_{i=1}^n (t_i - o_i)^2 \quad 4.2$$

$$RMSE = \sqrt{\frac{1}{n} \sum_{i=1}^n (t_i - o_i)^2} \quad 4.3$$

Where  $t_i$  implies the experimental output, also known as the target value, and  $o_i$  is the ANN forecasted value. Many research works (Castresana et al., 2021; Pitchaiah et al., 2023; Sayyed et al., 2021) have utilized MSE and RMSE as the loss function to be minimized and

for evaluating their model's performance due to their desirable properties of convexity, symmetry, and differentiability.

Another way to assess the prediction accuracy of the ANN model involves employing the coefficient of determination ( $R^2$ ), which is, in fact, the absolute fraction of variance, and it can be calculated using Equation 4.4. These metrics can offer valuable insights, according to similar studies (Aydın et al., 2020; Castresana et al., 2022; Işcan, 2020) into the model's ability to fit the data. If  $R^2$  approaches unity, the RMSE value becomes smaller, indicating that the model is capable of effectively learning patterns within the data.

$$R^2 = 1 - \left( \frac{\sum_{i=1}^n (t_i - o_i)^2}{\sum_{i=1}^n (o_i)^2} \right) \quad 4.4$$

#### 4.3.4 Data Allocation Ratio Selection

Before the implementation of the network, it is necessary to divide the data into train, test, and validation data. The training set is utilized for network training among these randomly selected datasets. In contrast, the test dataset is employed to assess the network's performance on unseen data, and the validation set is used to tune the hyperparameters of the network and prevent overfitting. Failing to pre-determine the percentage of data allocated to each set can lead to biased results and overfitting. The proportion of the allocated data for testing, training, and validation datasets depends on the specific problem, the dataset's size, and the modeling technique used in the neural network. Conferring to previous studies, a typical data partition involves allocating 70% for training, 15% for validation, and 15% for testing (Agarwal et al., 2013; Najafi et al., 2009). However, the best way to determine the percentage split is to experiment with different ratios and evaluate the model's performance on each split using appropriate metrics. This can help you choose the optimal split for your specific problem. In this regard, networks with random initial weights were selected, and different ratios were tested for them. Table 3 shows the result of this performance evaluation on different dataset splits for a multilayer perceptron network. This network has one hidden layer of 5 neurons using the *Tansig* transfer function. The performance metric used in this

regard is the Mean Squared Error (MSE), commonly used for regression problems, and a lower MSE indicates better performance of the model. As can be seen from Table 3, the lowest calculated error is when the model allocates 80% of the dataset for network training and evenly distributes the remaining 20% for testing and validation purposes.

Table 3 Network's performance for different dataset ratio allocations in MLP neural network

Network performance (MSE)	Validation data (%)	Test data (%)	Train data (%)
0.0021	30	30	40
0.0021	25	25	50
0.0010	20	20	60
8.02e-04	15	15	70
1.52e-04	10	10	80
1.70e-04	5	5	90

The performance of the radial basis function (RBF) neural network with ten hidden neurons and a radial basis function width of 1 was also evaluated on various dataset ratios. As seen from Table 4, the best ratio with the lowest MSE is when 70% of the dataset is allocated to the network's training, and the remaining 30% is equally divided for testing and validation purposes. The results of these two networks are presented in Figure 4. By comparing these results, we can see that the RBF network performs better than the MLP network. The best data split for the MLP and RBF networks is when 80% and 70% of the dataset are allocated for training, respectively, and the remaining is utilized equally to test and validate the network result.

Table 4 Network's performance for different dataset ratio allocation in RBF neural network

Network performance (MSE)	Validation data (%)	Test data (%)	Train data (%)
1.42e-4	30	30	40
4.52e-4	25	25	50
8.33e-05	20	20	60
7.94e-05	15	15	70
9.49e-05	10	10	80
2.18e-4	5	5	90

#### 4.4 THE ANN ARCHITECTURE

The architecture of a neural network encompasses the organization of the individual components that make up the network. It is crucial to select the optimal architecture for an artificial neural network to leverage its computational power and derive its maximum benefits. This research used the Multilayer Perceptron (MLP) and Radial Basis Function (RBF) neural networks to compare their performance and response time to determine the best-representing model among the various existing ANN approaches.

Selecting a suitable architecture for a neural network varies depending on the type of network in question. For a multilayer perceptron (MLP) network, the focus is on determining the arrangement of neurons into layers, selecting appropriate activation functions, and deciding on the optimal number of hidden neurons. On the contrary, the architecture selection of a radial basis function (RBF) neural network involves determining the appropriate number of hidden neurons, the spread or width of the RBFs, and the RBF activation function.

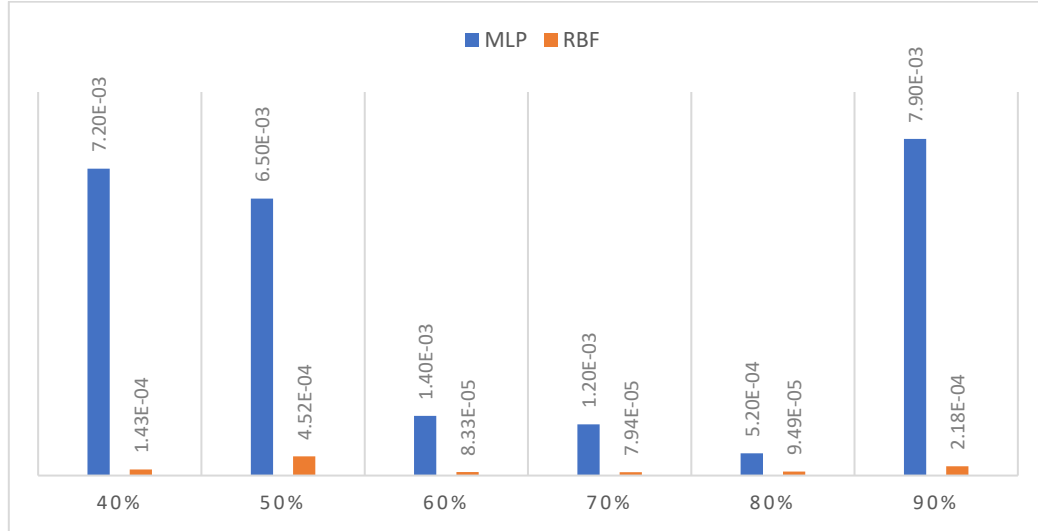


Figure 4 MSE comparison of the two neural networks for different training ratios

Overall, the architecture selection process involves making trade-offs between model complexity and performance, and various techniques can be used to determine the optimal architecture for a given problem.

#### 4.4.1 Execution of the MLP network model

As previously mentioned, the neural network's structure is typically determined by factors such as the number of hidden layers, the transfer functions within every layer, and the number of neurons, with all these elements significantly influencing the network's performance. To create this network in the MATLAB software environment, the neural network fitting tool is used (Figure 5), which uses an interactive way of developing neural networks by allowing the user to select the network architecture, data sets, and various network training options. There are no established guidelines for achieving the optimal topological structure in ANN, so a heuristic approach was employed during this stage. Following the design process, the ANN model's performance was evaluated by considering the coefficient of determination ( $R^2$ ) and mean squared error (MSE) as evaluative metrics.

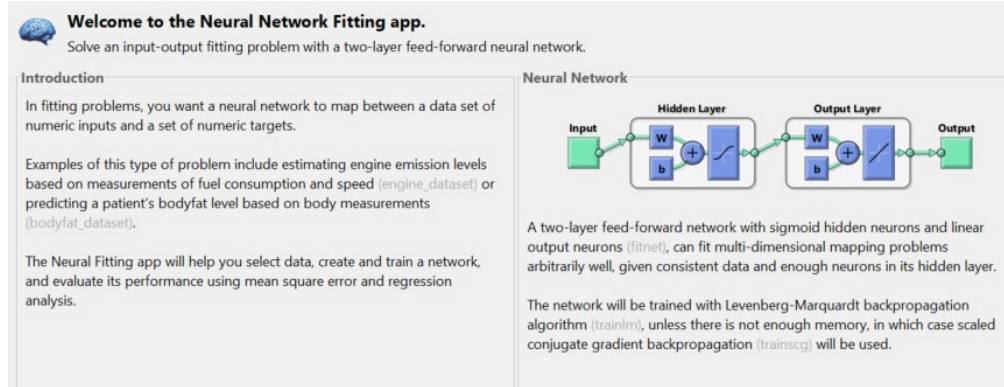


Figure 5 MATLAB neural network fitting tools

As seen in Figure 6, this network comprises a triple-layered structure: the input layer, hidden layer(s), and an output layer. The input layer has five neurons equal to the count of the best underperformance indicators determined in Chapter 3 and depicted in Figure 6. The output layer has one neuron, representing the engine's operating load. Regarding the number of hidden layers, Sözen and Arcaklioğlu (Sözen & Arcaklioğlu, 2005) recommended using two hidden layers. However, based on (Ismail et al., 2012; Najafi et al., 2009), a single hidden layer is also deemed enough for learning the data in regression problems. In general, a higher number of hidden layers may not improve performance as optimizing the network becomes more complex. If the dataset size is small, such as in our case, it would have no positive influence. Therefore, given the complexity and size of our dataset, a single hidden layer is used in this study as a rule of thumb, which is later adjusted in section 4.3.2 to evaluate its parametric effect on the network performance and to determine the optimal architecture. The activation function utilized for the hidden layer was '*Tansig*', whereas '*Purelin*' was employed for the output layer, as evident in Figure 6. The *Tansig* activation function finds widespread use in multilayer perceptron models because it is continuous, non-linear, and has bounded output values (Sharon et al., 2012). The dataset is utilized randomly for training, testing, and validating the network.

Regarding the training algorithm, a backpropagation algorithm (BPA) is widely utilized to train a feedforward neural network (FFNN). Still, it can get trapped in local minima and cannot identify the global minimum of the error function. As an alternative, the

Levenberg-Marquardt (LM) algorithm is faster and has superior convergence properties, demonstrating its effectiveness in forecasting the pertinent parameters of the engine (Yang et al., 2022). This algorithm displays outstanding performance for networks with a limited number of weights, usually a few hundred or less, and is notably advantageous compared to alternative algorithms when precise training is required (Beale et al., 2010).

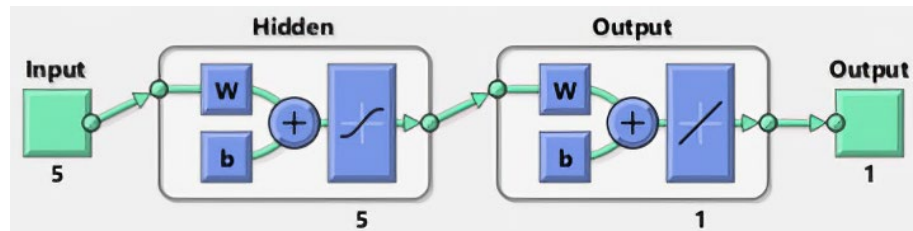


Figure 6 The block diagram in an MLP network implemented by MATLAB

#### Stopping criteria and practical considerations

Stopping criteria play a crucial role in training all neural networks, including the MLP model, by determining when to terminate the process to prevent overfitting. The most widely used stopping criteria include the minimum error threshold, maximum number of iterations, and validation error threshold. The minimum error threshold stops the training process when the error rate reaches a certain level, indicating that the network has achieved the desired level of accuracy. The MSE value in our study is set to 0, which is our desired target. The maximum number of iterations determines the point at which the training process ends, regardless of the error value. The training process in this study is limited to a maximum of 1000 iterations, meaning that the dataset will be presented 1000 times consecutively for the training process to take place, and if the number of iterations reaches 1000, the network operation will cease. The network has been configured to permit a maximum of 6 validation checks regarding the validation error threshold. The training process is halted once this limit is reached, and the neural network stops functioning. A validation test enables the neural network to withstand new data that could potentially increase network error.

Figure 7 shows the implemented MLP neural network structure in the MATLAB software environment.

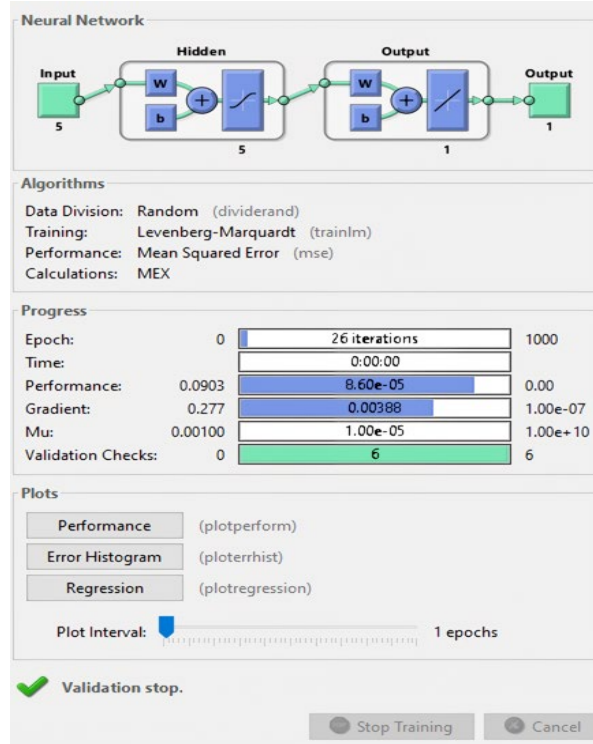


Figure 7 The structure of the implemented MLP neural network in MATLAB software.

In the progress section of Figure 7, information about the training process of the neural network is provided. All the factors in this section have an initial value and a final value, and if the network reaches this absolute value, the process will be stopped. “Epoch” represents one complete pass of the training dataset through the neural network, and it is set at 1000 for this study. “Time” shows the training duration, which is not limited to any value in this research. “Performance” represents the precision of the network based on the chosen performance metrics. In this study, the mean squared error (MSE) is the metric to evaluate network precision and is set to an initial value of 0. A lower MSE indicates better neural network performance in predicting the output values. “Gradient” represents the error’s partial derivatives about every weight and bias within the neural network. It updates the weights and biases through gradient descent, minimizing network error. In our training process, the initial gradient is set to  $1e-7$ . “Validation checks” is the maximum allowable number of failures before stopping the neural network training, which in this study is set at 6, and if exceeded, the training process is terminated.

#### 4.4.2 Modification of the MLP Structure

In this section, we will investigate the alterations to the MLP network structure and evaluate their influence on the output response to determine the optimal model. The tuned hyperparameters encompass the learning algorithm, the number of hidden layers, and the number of neurons within every hidden layer. As outlined in section 4.3.4, the optimal data split ratio for achieving the best network performance in the MLP model is to allocate 80% of the input data to the training process while evenly splitting the remaining 20% between the test and validation sets. As such, it is crucial to maintain this data split ratio unchanged when implementing any modifications to the network.

Table 5 Training algorithms and their corresponding function in MATLAB

<b>Algorithms</b>	<b>Training functions</b>
Levenberg–Marquardt backpropagation	Trainlm
Bayesian Regulation backpropagation	Trainbr
BFGS quasi-Newton backpropagation	Trainbfg
One step secant backpropagation.	Trainoss
Scaled conjugate gradient backpropagation.	Trainscg
Resilient backpropagation (Rprop)	Trainrp
Gradient descent with momentum backpropagation	Traingdm
Gradient descent backpropagation	Traingd
Gradient descent with momentum and adaptive learning backpropagation	Traingdx
Conjugate gradient backpropagation with Polak-Ribiere updates	Traincgp

## Training algorithms

This study examined various training algorithms for our Feedforward Neural Network (FFNN). The output parameter was tested after being trained by all the functions listed in Table 5. This analysis aimed to evaluate the neural network's performance and identify the most effective training algorithm for this specific application.

The FFNN was trained using various training functions listed in Table 5 and evaluated on a network with one hidden layer containing 10 neurons. The assessment is based on factors such as the number of epochs needed, as well as the root mean square error (RMSE) and correlation coefficient ( $R^2$ ). Table 6 shows the results of the network trained with various training functions using the same train, test, and validation input dataset.

Table 6 MLP model Evaluation using different training functions.

<b>Training function</b>	<b>Number of epochs</b>	<b>RMSE</b>	<b>(<math>R^2</math>)</b>
Trainlm	32	3.50E-02	9.85E-01
Trainbr	96	2.10E-02	9.94E-01
Trainbfg	11	1.70E-01	6.38E-01
Trainoss	26	2.00E-01	5.30E-01
Trainscg	13	1.80E-01	5.70E-01
Trainrp	21	1.90E-01	5.80E-01
Traingdm	46	3.40E-01	1.00E-01
Traingd	1000	2.00E-01	5.00E-01
Traingdx	31	3.60E-01	1.00E-01
Traincgp	12	1.60E-01	6.60E-01

Levenberg-Marquardt backpropagation and Bayesian Regulation backpropagation have demonstrated the best performance and highest correlation coefficient among various training functions. However, Levenberg-Marquardt, a second-order algorithm, utilizes the second derivative of the error function, unlike other algorithms, such as gradient descent, which uses only the first derivative. Despite the marginal superiority of the Bayesian Regulation backpropagation in performance, the ability of Levenberg-Marquardt backpropagation to converge faster to the minimum of the error function makes it a more suitable training algorithm for our neural network (Canakci et al., 2006; Mariani et al., 2014; Rezaei et al., 2015; Roy et al., 2014).

#### Number of hidden layers and neurons

In this section, experimentation was conducted to determine the best neural network configuration by assessing various numbers of neurons in its hidden layer. Typically, the power or capacity of a model can be enhanced by adding more hidden layers and neurons to the neural network. Nevertheless, selecting an excessive number of neurons in the hidden layer can pose practical difficulties. Aside from increasing the computational costs, an excessively high number of hidden neurons can potentially lead to model overfitting. Overfitting manifests when a model excels on the training data but yields inferior performance on new, previously unseen data, also known as test data (Goodfellow et al., 2016). Considering the intricacy of our network and the count of input and output variables, one hidden layer was sufficient and resulted in favorable outcomes. The network was trained with the Levenberg-Marquardt algorithm, and the input data used for training the dataset remained the same throughout all the experiments. Based on Figure 8 and Table 7, it can be observed that using 5 neurons in the hidden layer results in the highest coefficient of correlation and the smallest RMSE, with values of 0.998 and 0.012, respectively. Table 8 displays the details of the selected network with the best performance for our study.

Table 7 Network's performance for different numbers of hidden neurons

Learning algorithm	Network Structure	Training MSE	Testing MSE	Validation MSE	All data MSE	( $R^2$ )
LM	5-1-1	5.51E-03	7.43E-03	1.18E-03	5.24E-03	9.37E-01
LM	5-2-1	1.25E-03	2.29E-03	2.20E-05	1.23E-03	9.91E-01
LM	5-3-1	7.67E-04	6.21E-04	4.00E-05	6.70E-04	9.94E-01
LM	5-4-1	3.06E-04	3.93E-04	3.80E-04	3.24E-04	9.96E-01
LM	5-5-1	6.00E-05	9.49E-04	2.00E-06	1.52E-04	9.98E-01
LM	5-6-1	5.68E-04	6.97E-04	3.99E-04	5.64E-04	9.95E-01
LM	5-7-1	1.93E-04	4.91E-03	1.43E-03	8.55E-04	9.91E-01
LM	5-8-1	3.21E-03	3.54E-03	2.70E-03	3.20E-03	9.65E-01
LM	5-9-1	7.50E-05	2.33E-03	9.30E-05	3.29E-04	9.96E-01
LM	5-10-1	3.80E-05	1.09E-02	9.60E-05	1.25E-03	9.85E-01

#### 4.4.3 Results of the MLP Network

Using the empirical data, the MLP artificial neural network was constructed to forecast the operational load of the diesel engine generator. The input parameters of the network were Exhaust gas temperature, Sulfur (S), Carbon monoxide (CO), Carbon dioxide (CO<sub>2</sub>), and Oxygen(O<sub>2</sub>). The utilization of ANN for predicting the operational load of the DEG in the experimental engine demonstrated noteworthy performance metrics. This underscores the predictive capability of the developed network for the DEG's operational load. Figure 9 illustrates the performance of the network over 15 epochs. The plot shows that the train mean squared error (MSE) steadily decreases throughout training.

Table 8 Network attributes generated on MATLAB

MATLAB	
<b>Topology</b>	5 inputs, 1 output, 1 hidden layer with 5 hidden neurons (5-5-1)
<b>Data</b>	Training subset: 80% of the input data was selected randomly Test subset: 10% randomly selected input data Validation subset: 10% randomly selected input data
<b>Activation function</b>	Hyperbolic tangent sigmoid (Tansig)
<b>Training algorithm</b>	Levenberg–Marquardt
<b>Loss function</b>	Minimum MSE
<b>Stopping criteria</b>	Cease network training once the validation error begins to rise after 6 times.

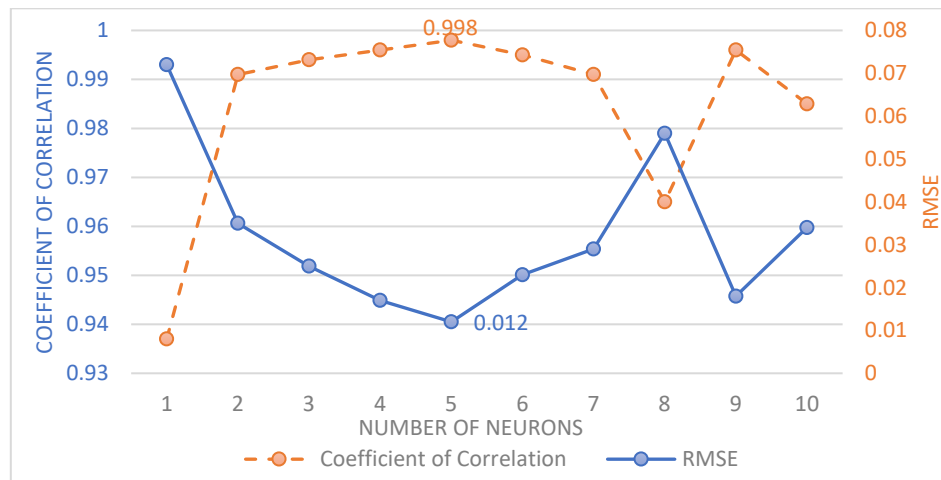


Figure 8 RMSE and coefficient of correlation for different numbers of neurons in MLP network.

Similarly, the validation MSE decreases in the initial epochs but increases after the ninth iteration. Overall, the network achieved the best validation performance at the ninth epoch, with an MSE of  $2.2973e-06$ . The training process terminates once the validation error rises after six consecutive iterations.

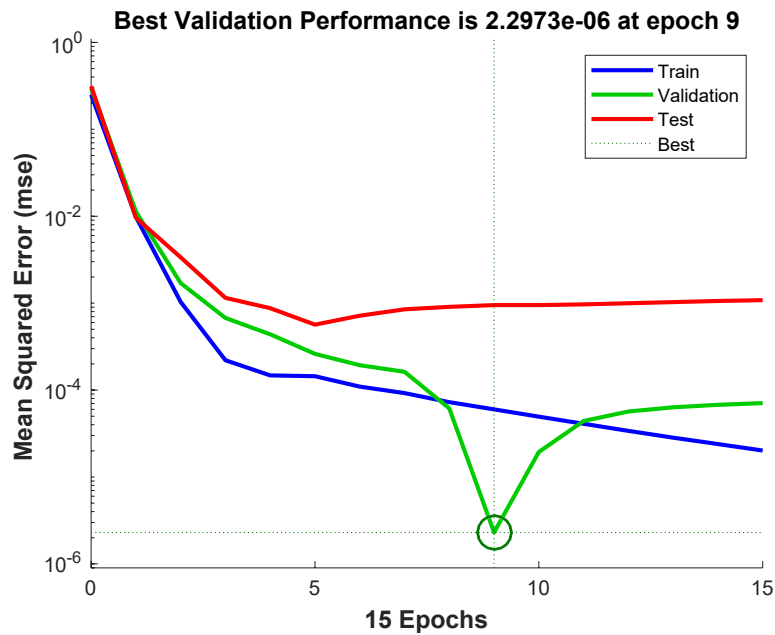


Figure 9 Performance plot of the MLP neural network

Figure 10 depicts the selected network architecture's correlation coefficient 'R' for the training data and the entire dataset. This coefficient is dependent on the network's performance and serves as a metric to evaluate it, with a value closer to 1 indicating a lower network error. The horizontal axis represents the target data for training the neural network, while the vertical axis represents the corresponding predictions the trained neural network generates. The graph should align closely with the T=Y line to ensure optimal network performance, which signifies that the output data closely matches the target value. This alignment indicates that the network accurately predicts the target values and performs its intended function. As can be seen from Figure 10, an acceptable level of correlation exists between the target output and the neural network output. This correlation signifies that the network has been trained well and can accurately predict the target values. The equation for the best linear fit that can accurately describe the output for both the training data and all data is equal to Equation (4.5) and (4.6) with the regression value of 0.99963 and 0.99916, respectively.

$$\text{Output} \sim = 1 * \text{Target} + 0.0031 \quad (4.5)$$

$$\text{Output} \sim = 0.99 * \text{Target} + 0.0092 \quad (4.6)$$

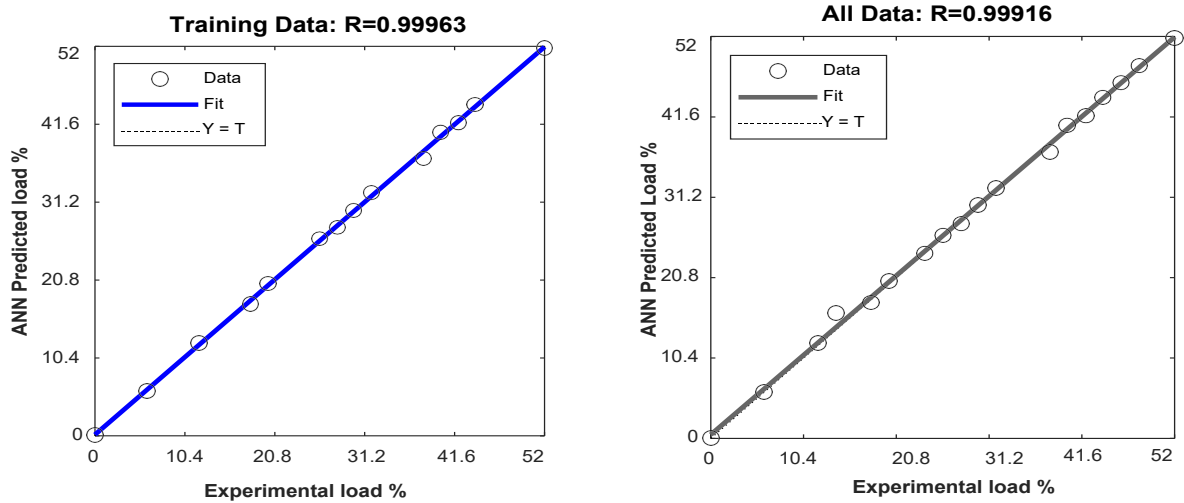


Figure 10 Regression plot of the ANN predicted operating load and the actual load value using MLP neural network.

Figure 11 illustrates the training progress of the neural network across 15 epochs, with the vertical axis indicating the points at which the network failed during this process. As can be seen, the network did not encounter any failures until epoch 9 during the 15 training epochs. However, as the number of validation checks was set at 6, the network stopped the training process after 6 consecutive failures.

#### 4.4.4 Execution of the RBF network model

In this section, we will discuss the implementation of the Radial Basis Function (RBF) network. The architecture of this network is determined by two key parameters: the count of neurons in the hidden layer and the width of the RBF, also known as the spread. These parameters play significant roles in the network's performance and must be carefully tuned to achieve optimal results. This network was implemented in MATLAB using the 'newrb' command. The data split in this network is also random, meaning that the data is randomly

selected for training, testing, and validation of the network. The neural network underwent training via the Levenberg-Marquardt algorithm (trainlm), and the model's performance was evaluated using the mean squared error (MSE) metric.

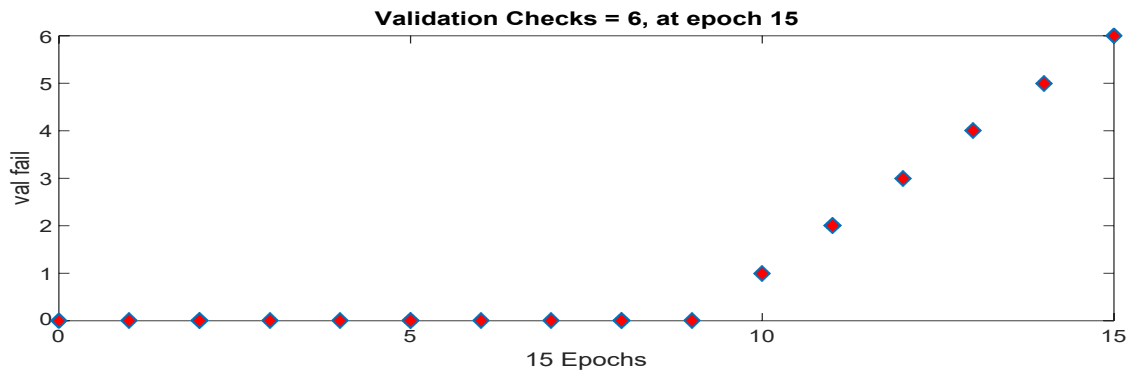


Figure 11 Training state of the MLP network

#### 4.4.4 Execution of the RBF network model

In this section, we will discuss the implementation of the Radial Basis Function (RBF) network. The architecture of this network is determined by two key parameters: the count of neurons in the hidden layer and the width of the RBF, also known as the spread. These parameters play significant roles in the network's performance and must be carefully tuned to achieve optimal results. This network was implemented in MATLAB using the 'newrb' command. The data split in this network is also random, meaning that the data is randomly selected for training, testing, and validation of the network. The neural network underwent training via the Levenberg-Marquardt algorithm (trainlm), and the model's performance was evaluated using the mean squared error (MSE) metric.

##### Stopping criteria

In this network architecture, the maximum number of training iterations was set to 1000 epochs, meaning that the data was presented 1000 times consecutively during the training process. Initially, a set of weights is generated and then updated using the 'Trainlm' algorithm to minimize the network's mean squared error. If the number of iterations reaches 1000, the

training process is stopped. The maximum number of validation failures has been set to 6, meaning the network training process will terminate after 6 unsuccessful iterations.

#### **4.4.5. Modification of the RBF network**

This section will examine the modifications applied to the RBF network framework and assess their impact on the output response to identify the most effective model. The adjusted hyperparameters comprise the Spread coefficient and the number of hidden neurons.

##### Spread coefficient

In implementing the Radial Basis Function (RBF) network, the width of the Gaussian function, known as the Spread parameter, is first determined because it is a critical hyperparameter in an RBF neural network. In case the spread coefficient is too small, the basis functions will become too narrow, leading to a situation where the network won't be able to capture the complex relationships between the inputs and outputs. In contrast, if the spread coefficient is excessively large, the basis functions will overlap considerably, making the network excessively flexible and susceptible to overfitting. As a result, selecting the suitable spread coefficient becomes imperative to guarantee that the RBF network can generalize well to unseen data and produce precise predictions. The optimal value of this parameter is obtained through trial and error based on the input data. Table 9 presents the mean squared error (MSE) results of the radial basis function (RBF) network for different values of the spread coefficient. The train, test, and validation data remain the same across all tests, with a maximum of 20 hidden neurons.

Based on the results presented in Table 9, the neural network model with a spread coefficient of 1 exhibits the lowest MSE of 1.51E-04, indicating superior performance among the evaluated models. Hence, this spread coefficient is chosen for our model.

Table 9 RBF network result with different spread coefficients

Spread Coefficient	Mean square error (MSE)
0.1	1.90E-03
0.3	9.00E-04
0.5	6.59E-04
0.7	2.25E-04
1	1.51E-04
1.2	0.000126

#### Hidden neurons' count

The optimal quantity of hidden neurons can significantly impact an RBF network's performance. The role of the hidden neurons is to transform the input domain into a higher-dimensional domain. Data in this space can be better separated and classified by the output neuron. In the event of too few hidden neurons, the network cannot generalize sufficiently and would be prone to underfitting. On the contrary, with excessive hidden neurons, the network would become susceptible to overfitting, resulting in poor performance on unseen data. The changes in the root mean squared error (RMSE) and coefficient of correlation as a function of the number of hidden neurons are illustrated in Figure 12. Based on the results, the network achieves its best performance with an RMSE of 0.00918 and a correlation coefficient 0.998 when the number of hidden neurons is set to 12. Thus, our network architecture is configured with 12 hidden neurons.

#### 4.4.6 Results of the RBF network

The RBF neural network has demonstrated excellent overall performance in predicting the operating load of the DEG based on the input parameters, and the network produced

highly accurate results with negligible error. The network's performance on the training data can be seen in Figure 13 as the number of neurons in the hidden layer increases. The mean squared error (MSE) decreases initially over the first 12 iterations, reaching an almost negligible value of  $1.53E-27$ , which is very close to the network's objective of zero error.

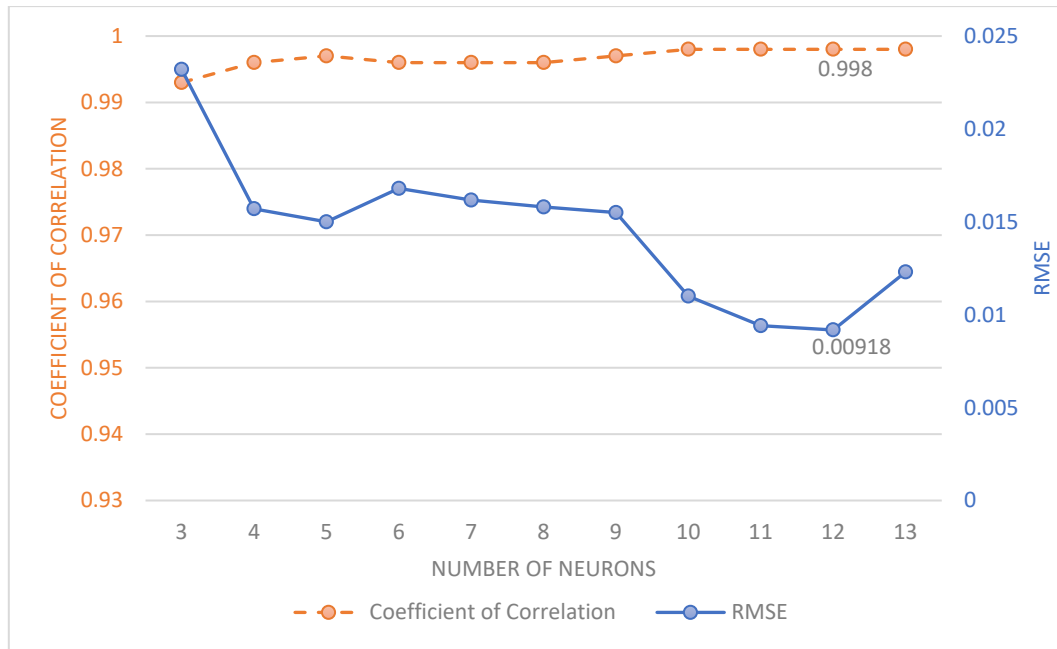


Figure 12 RMSE and coefficient of correlation for predicting the operating load in RBF network

Figure 14 illustrates the correlation coefficient 'R' for both the training data and the entire dataset. As shown in the figure, there is a satisfactory level of correlation between the target output and the neural network output. This correlation indicates that the network has been successfully trained and can accurately predict target values.

Figure 15 illustrates the training state of the network, where it can be observed that the network's performance on validation data declined for six consecutive iterations after 12 epochs, ultimately leading to the termination of the network's training process.

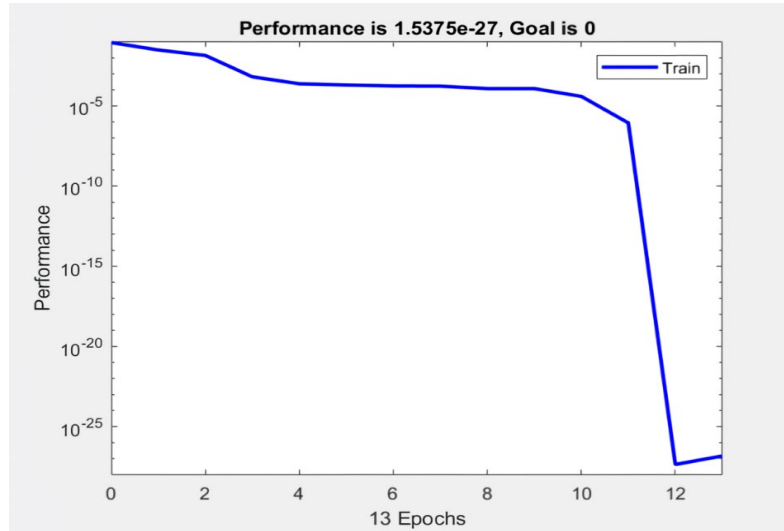


Figure 13 RBF network performance in different iterations

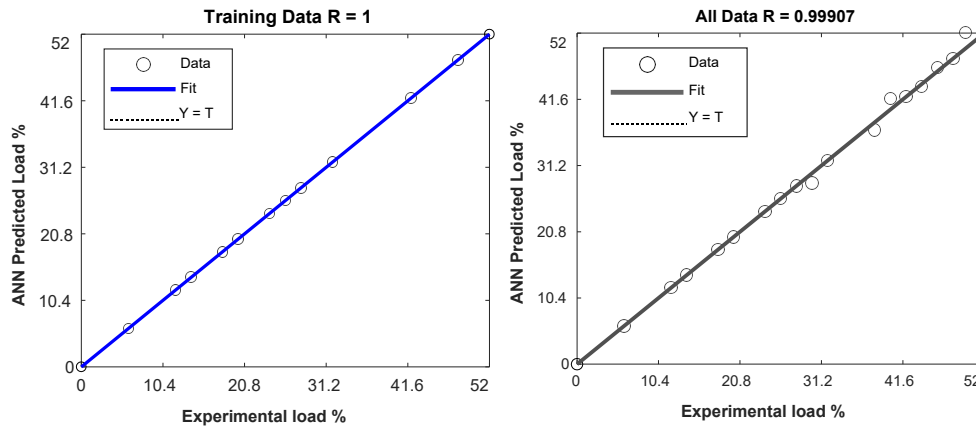


Figure 14 Regression plot of the ANN predicted operating load and the actual load value using RBF neural network.

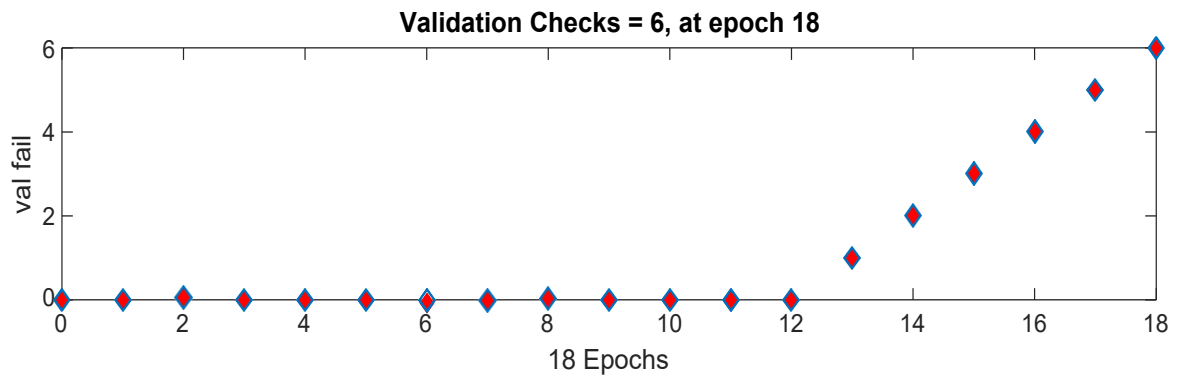


Figure 15 Training state of the RBF network



## CHAPTER 5: RESULTS AND DISCUSSIONS

The results of the MLP and RBF predictions for our diesel engine generator's operating load are presented in Table 10. The results indicate that both networks have effectively learned the correlation between inputs and targets. Additionally, when comparing the neural network prediction and empirical data, it is evident that the ANN can accurately model the diesel engine's operating load with minimal training data. This proposed ANN approach can be employed to detect the underperformance of the diesel engine. While demonstrating nearly similar performance, the MLP network requires fewer neurons, generates less complex output equations, resulting in shorter processing times, and is consequently chosen for our optimization problem.

Table 10 RMSE and  $R^2$  comparison between MLP and RBF for DEG operating load prediction

	MLP			RBF		
	Train data	Test data	All data	Train data	Test data	All data
$R^2$	0.99	0.98	0.99	0.99	0.976	0.99
RMSE	0.007	0.03	0.012	3.83E-14	0.023	0.012

### 5.1 APPLICATION OF THE PROPOSED NETWORK FOR DEG OPTIMIZATION

After choosing the best network architecture for our neural network, this network can now be implemented on our diesel engine generator to determine whether it is underperforming. As pictured in Figure 16, this is done by acquiring the emission data from the flue gas analyzer and similar to all function approximation problems, the developed MLP network can generalize from the provided input-output pairs to predict the operating load for new, unseen data inputs. In case of underperformance, a load bank is used to apply a load on the generator part of the DEG in addition to our demand side, thereby mitigating the negative impacts of operating at a low load by converting the excess electrical energy into heat.



Figure 16 Data acquisition for the neural network

As per the manufacturer, Caterpillar, if the engine operates at a load below 30% of its nominal power, it is deemed to be underperforming (Jabeck, 2013). Consequently, as illustrated in Figure 17, should our DEG operate below 90 kW, the proportional control system in MATLAB/Simulink introduces resistive loads into our system to prevent the engine's underperformance. The load banks can alternatively be switched manually by a supervisor once our neural network confirms the DEG underperformance.

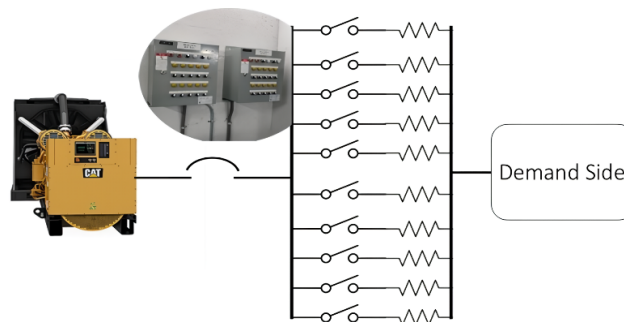


Figure 17 Resistive load bank control

The flow chart in Figure 18 illustrates the steps taken for the DEG optimization should it work below par, and its value is represented by  $P_{Ref}$  and Figure 19 shows the implemented schematic.

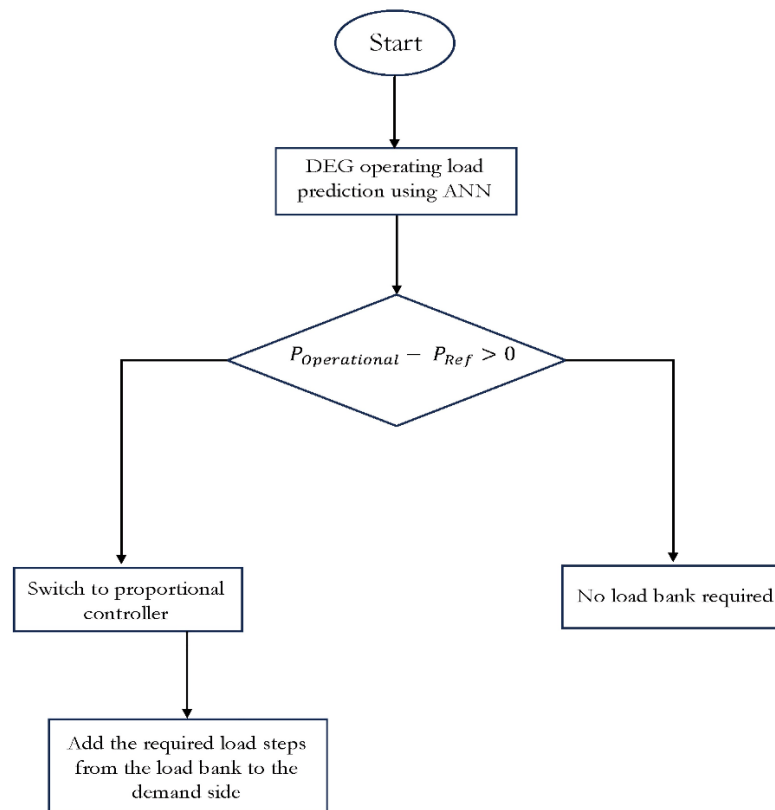


Figure 18 Optimization flow chart for our diesel engine generator

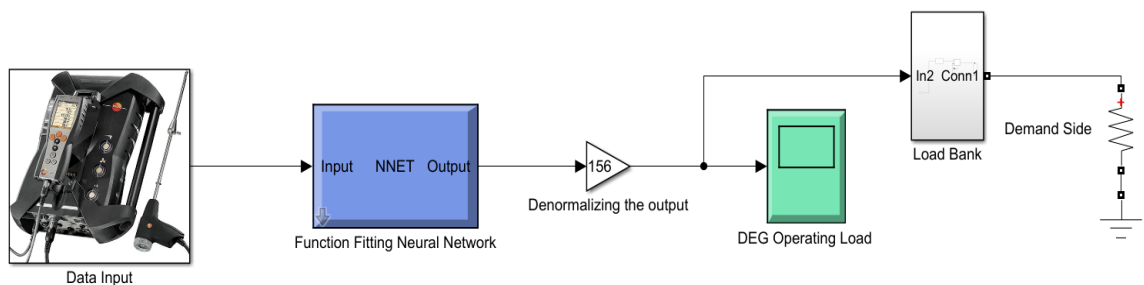


Figure 19 DEG Underperformance optimization schematic

In evaluating the underperformance optimization of the DEG, two scenarios are considered based on initially conducted experiments. This involves measuring exhaust gas temperature, along with emissions such as Sulfur (S), Carbon Monoxide (CO), Carbon Dioxide (CO<sub>2</sub>), and Oxygen (O<sub>2</sub>), which are then inputted to our developed neural network. If the neural network identifies that the DEG is performing below par, it will take corrective action through the control system by adding the necessary loads to the generator. The utilization of a load bank serves as a prevalent strategy to mitigate the adverse effects of underperformance, particularly in North America (Issa et al., 2020). Typically, a load bank operates as an automatically controlled resistor, applying a load to the generator unit of the DEG. This loading process converts electrical energy into heat energy, thereby improving the operational state of the diesel engine. This elevation in operating temperature prevents the formation of carbon deposits on injectors, valves, and the combustion chamber surface, along with addressing other associated problems like wet stacking.

### **5.1.1 Scenario 1**

In our initial scenario, we utilized data collected from our Diesel Engine Generator (DEG) while operating at 24% of its designated load capacity, which is considered low load operation for our generator (Table 11). This acquired dataset was subsequently input into our neural network, and upon denormalizing the network's output, it revealed that the generator was operating at 25% of its nominal power, showcasing an impressively precise estimate with a minimal margin of error.

After the neural network assesses the DEG's operation at 25% of nominal power, equivalent to 75kW in our generator, the control system introduces three 5kW loads from the load bank to prevent the generator's underperformance.

Table 11 Exhaust gas data from DEG operating at 24% of nominal power capacity.

Exhaust gas Temperature (°C)	Sulfur (S) (ppm)	Carbon monoxide (CO) (ppm)	Carbon dioxide (CO <sub>2</sub> ) (%)	Oxygen (O <sub>2</sub> ) (%)
312	0.1	277	196	162

### 5.1.2 Scenario 2

In our second scenario, the acquired exhaust dataset was collected while the DEG was operating at 38% of its nominal power, a zone considered to fall within the normal operating range (Table 12). Similar to the first scenario, this data was fed into our neural network, revealing that the generator was operating at 38.32% of its nominal power, which is a very accurate prediction similar to the first scenario. As the generator operates at a normal operating zone, the control system does not add any load steps from the load bank.

Table 12 Exhaust gas data from DEG operating at 38% of nominal power capacity

Exhaust gas Temperature (°C)	Sulfur (S) (ppm)	Carbon monoxide (CO) (ppm)	Carbon dioxide (CO <sub>2</sub> ) (%)	Oxygen (O <sub>2</sub> ) (%)
330	0.1	132	150	93

Overall, the utilization of Artificial Neural Network (ANN) models for predicting DEG attributes, including exhaust emissions, operational load, and performance, has been explored and contrasted with traditional statistical analyses such as regression models in many studies (Domínguez-Sáez et al., 2018; Tosun et al., 2016). These investigations consistently highlight the superior predictive capabilities of ANN models in understanding and forecasting the engine's behavior. Moreover, across multiple similar studies, it has been consistently noted that regression models fall short in accuracy compared to ANN models and they are a lot more time consuming (Tosun et al., 2017). The key observation is that achieving nearly acceptable results from regression models necessitates a substantial increase in the volume of data input to enhance prediction performance, which is not feasible in our study. On the other hand, among various studies that have used ANN models for predicting dynamic behavior of diesel engine generators, they were all centered on predicting attributes such as exhaust emissions, operating temperature, brake power, torque and overall engine performance. These predictions are mostly based on diverse input parameters including speed, fuel blend ratio, load, etc. (Fang et al., 2022; Ganesan et al., 2015; Ghobadian et al., 2009). However, it is noteworthy that, in the reviewed studies, there was a conspicuous absence of ANN applications for the detection and prevention of underperformance in diesel engine generators, which was the main motive behind our research, and this makes a distinct contribution to the existing body of research, addressing a critical gap. Such an approach represents a substantial step forward in tackling operational challenges and advancing the state-of-the-art in this field.

## CHAPTER 6: CONCLUSIONS

### 6.1 SUMMARY AND CONCLUSIONS

Diesel engine generators (DEGs) are pivotal in electrifying remote regions disconnected from the national electricity grid owing to their notable benefits, including simple operation, quick deployment, flexibility in handling varying demands, cost-effectiveness, and durability and reliability. However, one of the main challenges in using this type of generator has always been associated with the time when the electricity demand is low and the engine has to work for extended periods below its optimal level, which can damage the engine and shorten its lifespan by the emergence of adverse phenomena such as wet stacking, cylinder polishing, and cylinder glazing. Additionally, accurately identifying when a diesel engine generator is underperforming is another hurdle in the operation of DEGs. This research has leveraged exhaust gas data to train a neural network capable of predicting and pre-emptively addressing underperformance issues.

The initial chapter of this research delves into the imperative role of DEGs in the electrification of remote areas by drawing on the previous research conducted in this domain. This chapter also explores the challenges in the literature posed by DEGs' underperformance, particularly during periods of low demand, shedding light on the critical importance of addressing this issue for reliable and more cost-effective energy access in such regions.

The second chapter is a published article in *Energies* journal titled "Experimental Underperformance Detection of a Fixed-Speed Diesel–Electric Generator Based on Exhaust Gas Emissions". This article is dedicated to data collection process from the diesel engine generator in three separate tests under various load levels ranging from 0% to 52% of the engine's nominal output power, which is the first objective of our research. The recorded parameters include exhaust emission characteristics such as S, SO<sub>2</sub>, CO, CO<sub>2</sub> NO<sub>x</sub>, and O<sub>2</sub>, as well as exhaust gas temperature and Brake Specific Fuel Consumption (BSFC). Following the data collection, a thorough analysis was conducted to identify parameters exhibiting

consistent behavior under low-load conditions. These parameters were recognized as the most reliable underperformance indicators, and they were subsequently utilized in subsequent chapters to train the neural network, enabling it to identify when the engine is underperforming.

In the third chapter, we undertake a comparative analysis of different ANN models in industrial control settings and how they are practically employed as practical computational tools in non-linear operations compared to statistical forecasting methods like multiple regression. The limitations of regression models compared to their ANN counterparts are explored, showcasing how regression models can struggle to handle complex and non-linear patterns in the data, and they usually require significant number of assumptions in advance while ANNs do not have these limitations and because of having better generalization capacity, they can perform better on unseen datasets and produce more robust models. The subsequent section of the chapter looks into different ANN classifications, providing a comparative assessment of the advantages, drawbacks, and applications associated with each architecture. This classification is mainly centered on the learning algorithms and architectures of ANNs. It was demonstrated how the use of Feedforward Neural Networks (FFNN) such as Multilayer Perceptron (MLP) and Radial Basis Function (RBF) are widely used in similar contexts in forecasting the diesel engine generator's behavior such as exhaust emissions, fuel consumption, etc. mainly because of their robustness under different datasets and their training capability for diverse input-output mappings. The other FFNN models, such as Convolutional Neural Networks (CNN), were also investigated, proving not to be in line with the scope of our research problem as they are primarily used in other applications such as image classification, object detection, and face detection. The other large classification of ANN models, namely, Recurrent Neural Networks (RNN), was also explored, demonstrating that because of the unique architecture of these neural networks, they are primarily used in contexts where we have sequential data and the network needs to retain past inputs to produce accurate results. Consequently, they are more utilized in Natural Language Processing (NLP) applications where the temporal order of inputs is essential. That is why, by the review of the literature, these networks are found to be less utilized in

regression problems, especially in industrial settings and, more specifically, diesel engine generator's dynamic behavior forecasting. A comprehensive analysis of the existing architectures in the literature reveals that Multilayer Perceptron (MLP) neural networks, which in many studies are referred to as Feedforward Neural Networks (FFNN), along with Radial Basis Function (RBF) networks, are the most widely used architecture in dynamic behavior forecasting of diesel engine generators and they are chosen for this study because of their accuracy, time efficiency, and robust performance across different datasets.

In the fourth chapter of this study, we embark on creating an artificial neural network using MATLAB's neural network toolbox, a pivotal step in our research. This process involves data preprocessing, which includes normalizing our input data to enhance the convergence and stability of the neural network during the training process. The next step requires dataset allocation for train, test, and validation data, where different dataset splits are tested to find the one that yields the most accurate results. After simulating the ANN models, each network's hyperparameters, including the training algorithm, number of hidden layers, neurons, and iterations, are modified, and their respective error is calculated and illustrated.

The fifth chapter delves into the yielded results of both MLP and RBF networks, comparing their performance and accuracy in learning the nonlinear behavior of input data and how well it performs on unseen data to predict the operating load of the engine. This implemented neural network is then utilized in a proportional control system through MATLAB/ Simulink that decides on the value of the resistive load that needs to be added to the generator part of the DEG to change its operating load reaching to the minimum operational load prescribed by the manufacturer. This process converts excess electrical power to heat, consequently increasing the engine's temperature and preventing the formation of carbon deposits inside the engine. This proactive measure is crucial in avoiding potential adverse consequences to the engine. Two separate scenarios are then tested on the control system to verify its responsiveness when the engine is performing below par and operating in its optimal operational range.

## **6.2 THE LIMITATIONS OF THE MODEL, RECOMMENDATIONS, AND FUTURE RESEARCH**

In this research, a notable challenge in diesel engine generator optimization lies in accurately predicting underperformance. This issue has been successfully tackled with remarkable precision by applying artificial neural networks. Nevertheless, it is equally vital to implement preventative measures after the load prediction step. Load banks often fulfill this purpose, especially in North America, with the goal of preventing potential negative consequences. This study has employed this method to tackle the issue, albeit with the trade-off of heightened fuel consumption, increased electricity costs, and elevated pollution. Nevertheless, despite its limitations, this approach still offers some advantages compared to other alternatives. One alternative involves utilizing a combination of small diesel generator sets, where the combined output power equals that of a single large diesel engine generator. However, this proves to be a significantly more expensive approach when compared to the utilization of load banks.

In future studies, more sustainable alternatives can be researched and employed, such as hybridizing the DEG with renewable energy sources such as wind turbines to prevent the low-load operation of the engine, especially for extended periods.

## BIBLIOGRAPHIC REFERENCES

- Agarwal, A. K., Srivastava, D. K., Dhar, A., Maurya, R. K., Shukla, P. C., & Singh, A. P. (2013). Effect of fuel injection timing and pressure on combustion, emissions and performance characteristics of a single cylinder diesel engine. *Fuel*, *111*, 374-383.
- Akbas, B., Kocaman, A. S., Nock, D., & Trotter, P. A. (2022). Rural electrification: An overview of optimization methods. *Renewable and Sustainable Energy Reviews*, *156*, 111935.
- Alexander, D. (2020). *Neural Networks: History and Applications*. Nova Science Publishers, Incorporated. <https://books.google.ca/books?id=6p18zQEACAAJ>
- Alloghani, M., Al-Jumeily, D., Mustafina, J., Hussain, A., & Aljaaf, A. J. (2020). A systematic review on supervised and unsupervised machine learning algorithms for data science. *Supervised and unsupervised learning for data science*, 3-21.
- Arriaga, M., Cañizares, C. A., & Kazerani, M. (2014). Northern lights: Access to electricity in Canada's northern and remote communities. *IEEE Power and Energy Magazine*, *12*(4), 50-59.
- Aydın, M., Uslu, S., & Çelik, M. B. (2020). Performance and emission prediction of a compression ignition engine fueled with biodiesel-diesel blends: A combined application of ANN and RSM based optimization. *Fuel*, *269*, 117472.
- Ayodele, T., Ogunjuyigbe, A., & Akinola, O. (2017). n-split generator model: An approach to reducing fuel consumption, LCC, CO<sub>2</sub> emission and dump energy in a captive power environment. *Sustainable Production and Consumption*, *12*, 193-205.
- Beale, M. H., Hagan, M. T., & Demuth, H. B. (2010). Neural network toolbox. *User's Guide, MathWorks*, *2*, 77-81.
- Canada, N. R. (2018). *The Atlas of Canada - Remote Communities Energy Database*. (NRCan). Retrieved 10 January 2023 from <https://atlas.gc.ca/rced-bdece/en/index.html>
- Canakci, M., Erdil, A., & Arcaklioğlu, E. (2006). Performance and exhaust emissions of a biodiesel engine. *Applied Energy*, *83*(6), 594-605.
- Castresana, J., Gabiña, G., Martin, L., Basterretxea, A., & Uriondo, Z. (2022). Marine diesel engine ANN modelling with multiple output for complete engine performance map. *Fuel*, *319*, 123873.

- Castresana, J., Gabina, G., Martin, L., & Uriondo, Z. (2021). Comparative performance and emissions assessments of a single-cylinder diesel engine using artificial neural network and thermodynamic simulation. *Applied Thermal Engineering*, 185, 116343.
- CER. (2018). *Market Snapshot: Overcoming the challenges of powering Canada's off-grid communities*. Canada Energy Regulator. Retrieved 7 January 2023 from <https://www.cer-rec.gc.ca/en/data-analysis/energy-markets/market-snapshots/2018/market-snapshot-overcoming-challenges-powering-canadas-off-grid-communities.html>
- Dike, H. U., Zhou, Y., Deverasetty, K. K., & Wu, Q. (2018). Unsupervised learning based on artificial neural network: A review. 2018 IEEE International Conference on Cyborg and Bionic Systems (CBS),
- Djelailia, O., Kelaiaia, M. S., Labar, H., Necaibia, S., & Merad, F. (2019). Energy hybridization photovoltaic/diesel generator/pump storage hydroelectric management based on online optimal fuel consumption per kWh. *Sustainable Cities and Society*, 44, 1-15.
- Domínguez-Sáez, A., Rattá, G. A., & Barrios, C. C. (2018). Prediction of exhaust emission in transient conditions of a diesel engine fueled with animal fat using Artificial Neural Network and Symbolic Regression. *Energy*, 149, 675-683.
- Fang, X., Papaioannou, N., Leach, F., & Davy, M. H. (2021). On the application of artificial neural networks for the prediction of NO x emissions from a high-speed direct injection diesel engine. *International Journal of Engine Research*, 22(6), 1808-1824.
- Fang, X., Zhong, F., Papaioannou, N., Davy, M. H., & Leach, F. C. (2022). Artificial neural network (ANN) assisted prediction of transient NOx emissions from a high-speed direct injection (HSDI) diesel engine. *International Journal of Engine Research*, 23(7), 1201-1212.
- Ganesan, P., Rajakarunakaran, S., Thirugnanasambandam, M., & Devaraj, D. (2015). Artificial neural network model to predict the diesel electric generator performance and exhaust emissions. *Energy*, 83, 115-124.
- German-Galkin, S., Tarnapowicz, D., Matuszak, Z., & Jaskiewicz, M. (2020). Optimization to limit the effects of underloaded generator sets in stand-alone hybrid ship grids. *Energies*, 13(3), 708.
- Ghobadian, B., Rahimi, H., Nikbakht, A., Najafi, G., & Yusaf, T. (2009). Diesel engine performance and exhaust emission analysis using waste cooking biodiesel fuel with an artificial neural network. *Renewable Energy*, 34(4), 976-982.

- Goga, G., Mahla, S. K., Chauhan, B. S., Yadav, A. S., Chakroborty, S., Garg, J., & Garg, S. B. (2023). Predication of performance and emissions characteristics adual fuel engine energized with liquid and gaseous materials by Artificial neural network. *Materials Today: Proceedings*.
- Goodfellow, I., Bengio, Y., & Courville, A. (2016). *Deep learning*. MIT press.
- Hewamalage, H., Bergmeir, C., & Bandara, K. (2021). Recurrent neural networks for time series forecasting: Current status and future directions. *International Journal of Forecasting*, 37(1), 388-427.
- Hoang, A. T., Nižetić, S., Ong, H. C., Tarelko, W., Le, T. H., Chau, M. Q., & Nguyen, X. P. (2021). A review on application of artificial neural network (ANN) for performance and emission characteristics of diesel engine fueled with biodiesel-based fuels. *Sustainable Energy Technologies and Assessments*, 47, 101416.
- Işcan, B. (2020). ANN modeling for justification of thermodynamic analysis of experimental applications on combustion parameters of a diesel engine using diesel and safflower biodiesel fuels. *Fuel*, 279, 118391.
- Ismail, H. M., Ng, H. K., Queck, C. W., & Gan, S. (2012). Artificial neural networks modelling of engine-out responses for a light-duty diesel engine fuelled with biodiesel blends. *Applied Energy*, 92, 769-777.
- Issa, M., Ibrahim, H., Hosni, H., Ilinca, A., & Rezkallah, M. (2020). Effects of low charge and environmental conditions on diesel generators operation. *Eng*, 1(2), 137-152.
- Jabeck, B. (2013). *The Impact of Generator Set Underloading (Caterpillar)*. Retrieved 2022-2-1 from [https://www.cat.com/en\\_US/by-industry/electric-power/Articles/White-papers/the-impact-of-generator-set-underloading.html](https://www.cat.com/en_US/by-industry/electric-power/Articles/White-papers/the-impact-of-generator-set-underloading.html)
- Jabeck, B. (October 2013). *The Impact Of Generator Set Underloading*. Retrieved 2022-01-14 from [https://www.cat.com/en\\_US/by-industry/electric-power/Articles/White-papers/the-impact-of-generator-set-underloading.html](https://www.cat.com/en_US/by-industry/electric-power/Articles/White-papers/the-impact-of-generator-set-underloading.html)
- Kshirsagar, C. M., & Anand, R. (2017). Artificial neural network applied forecast on a parametric study of Calophyllum inophyllum methyl ester-diesel engine out responses. *Applied Energy*, 189, 555-567.
- Liao, J., Hu, J., Yan, F., Chen, P., Zhu, L., Zhou, Q., Xu, H., & Li, J. (2023). A comparative investigation of advanced machine learning methods for predicting transient emission characteristic of diesel engine. *Fuel*, 350, 128767.

- Mariani, F., Grimaldi, C., & Battistoni, M. (2014). Diesel engine NOx emissions control: An advanced method for the O2 evaluation in the intake flow. *Applied Energy*, *113*, 576-588.
- McFarlan, A. (2018). Techno-economic assessment of pathways for electricity generation in northern remote communities in Canada using methanol and dimethyl ether to replace diesel. *Renewable and Sustainable Energy Reviews*, *90*, 863-876.
- Memon, S. A., & Patel, R. N. (2021). An overview of optimization techniques used for sizing of hybrid renewable energy systems. *Renewable Energy Focus*, *39*, 1-26.
- Mobarra, M., Rezkallah, M., & Ilinca, A. (2022). Variable Speed Diesel Generators: Performance and Characteristic Comparison. *Energies*, *15*(2), 592.
- Mustayen, A., Rasul, M., Wang, X., Negnevitsky, M., & Hamilton, J. (2022). Remote areas and islands power generation: A review on diesel engine performance and emission improvement techniques. *Energy Conversion and Management*, *260*, 115614.
- Mustayen, A., Wang, X., Rasul, M., Hamilton, J., & Negnevitsky, M. (2021). Theoretical investigation of combustion and performance analysis of diesel engine under low load conditions. IOP Conference Series: Earth and Environmental Science,
- Najafi, G., Ghobadian, B., Tavakoli, T., Buttsworth, D., Yusaf, T., & Faizollahnejad, M. (2009). Performance and exhaust emissions of a gasoline engine with ethanol blended gasoline fuels using artificial neural network. *Applied Energy*, *86*(5), 630-639.
- Penny, M. A., & Jacobs, T. J. (2016). Efficiency improvements with low heat rejection concepts applied to diesel low temperature combustion. *International Journal of Engine Research*, *17*(6), 631-645.
- Pitchaiah, S., Juchelková, D., Sathyamurthy, R., & Atabani, A. (2023). Prediction and performance optimisation of a DI CI engine fuelled diesel–Bael biodiesel blends with DMC additive using RSM and ANN: Energy and exergy analysis. *Energy Conversion and Management*, *292*, 117386.
- Rezaei, J., Shahbakhti, M., Bahri, B., & Aziz, A. A. (2015). Performance prediction of HCCI engines with oxygenated fuels using artificial neural networks. *Applied Energy*, *138*, 460-473.
- Rezkallah, M. (2016). *Design and control of standalone and hybrid standalone power generation systems* [École de technologie supérieure].

- Roy, S., Banerjee, R., & Bose, P. K. (2014). Performance and exhaust emissions prediction of a CRDI assisted single cylinder diesel engine coupled with EGR using artificial neural network. *Applied Energy*, *119*, 330-340.
- Royer, J. (2011). Status of remote/off-grid communities in Canada. *Natural Resources Canada*, *28*, 4626-4639.
- Sayed, S., Das, R. K., & Kulkarni, K. (2021). Performance assessment of multiple biodiesel blended diesel engine and NOx modeling using ANN. *Case Studies in Thermal Engineering*, *28*, 101509.
- Shams, S. R., Jahani, A., Kalantary, S., Moeinaddini, M., & Khorasani, N. (2021). The evaluation on artificial neural networks (ANN) and multiple linear regressions (MLR) models for predicting SO<sub>2</sub> concentration. *Urban Climate*, *37*, 100837.
- Sharon, H., Jayaprakash, R., Sundaresan, A., & Karuppasamy, K. (2012). Biodiesel production and prediction of engine performance using SIMULINK model of trained neural network. *Fuel*, *99*, 197-203.
- Shirneshan, A., Hosseinzadeh Samani, B., & Nedayali, A. (2022). Artificial neural network model to predict the performance of a diesel power generator fueled with biodiesel. *Engine Research*, *42*(42), 43-50.
- Sözen, A., & Arcaklioğlu, E. (2005). Solar potential in Turkey. *Applied Energy*, *80*(1), 35-45.
- Sutton, R. S., & Barto, A. G. (2018). *Reinforcement learning: An introduction*. MIT press.
- Tosun, E., Aydin, K., & Bilgili, M. (2016). Comparison of linear regression and artificial neural network model of a diesel engine fueled with biodiesel-alcohol mixtures. *Alexandria Engineering Journal*, *55*(4), 3081-3089.
- Tosun, E., Aydin, K., Merola, S. S., & Irimescu, A. (2017). Estimation of operational parameters for a direct injection turbocharged spark ignition engine by using regression analysis and artificial neural network. *Thermal Science*, *21*(1 Part B), 401-412.
- Tufte, E. D. (2014). *Impacts of low load operation of modern four-stroke diesel engines in generator configuration* [Institut for marin teknikk].
- Yang, R., Yan, Y., Sun, X., Wang, Q., Zhang, Y., Fu, J., & Liu, Z. (2022). An artificial neural network model to predict efficiency and emissions of a gasoline engine. *Processes*, *10*(2), 204.